TOPICAL REVIEW

Enabling Predication of the Deep Learning Algorithms for Low-Dose CT Scan Image Denoising Models: A Systematic Literature Review

MUHAMMAD ZUBAIR [1], **HELMI B. MD RAIS**[1], **FASEE ULLAH** [1], **QASEM AL-TASHI**[2], **MUHAMMAD FAHEEM**[3], **AND ARFAT AHMAD KHAN**[4]

[1]Institute of Emerging Digital Technologies (EDiT) and Center for Cyber Physical Systems (C2PS), Universiti Teknologi PETRONAS, Seri Iskandar 32160, Malaysia
[2]Department of Imaging Physics, The University of Texas MD Anderson Cancer Center, Houston, TX 77030, USA
[3]School of Computing (Innovations and Technology), University of Vaasa, 65200 Vaasa, Finland
[4]Department of Computer Science, College of Computing, Khon Kaen University, Khon Kaen 40002, Thailand

Corresponding author: Muhammad Zubair (muhammad_22000228@utp.edu.my)

ABSTRACT Computed Tomography (CT) is a non-invasive imaging modality used to detect abnormalities in the human body with high precision. However, the electromagnetic radiation emitted during CT scans poses health risks, potentially leading to the development of metabolic abnormalities and genetic disorders, which increase the risk of cancer. The Low-Dose CT (LDCT) scanning technique was developed to address these hazards, but it has several limitations, including noise, artifacts, reduced contrast, and structural changes. These drawbacks significantly reduce the diagnostic capabilities of Computer-Aided Diagnosis (CAD) systems. Eliminating these noises and artifacts while preserving critical features poses a significant challenge. Traditional CT denoising algorithms struggle with edge blurring and high computational costs, often generating artifacts in flat regions as noise levels increase. Consequently, deep learning-based methods have emerged as a promising solution for LDCT image denoising. In this study, a comprehensive Systematic Literature Review (SLR) following PRISMA guidelines was conducted to explore the latest advancements in deep learning algorithms for LDCT image denoising. This SLR spans LDCT image-denoising research from 2018 to 2024, providing a detailed summary of methodologies, benefits, limitations, parameters, and trends. This study delves into the acquisition process of CT scans, investigating radiation absorption across various anatomical regions, as well as identifying sources of noise and its distribution within the LDCT images. Additionally, it enhances our understanding of LDCT image denoising trends and provides valuable insights for future research, thus making a substantial contribution to ongoing efforts to enhance the quality and reliability of LDCT images.

INDEX TERMS Deep learning, image enhancement, image reconstruction, low dose CT image denoising, medial images denoising, noise removal techniques, systematic literature review.

GRAPHICAL ABSTRACT
Deep learning based LDCT image denoising models are searched in online databases based on the keywords. Subsequently, PRISMA has applied and selected 62 articles to address three specific research questions as given in **FIGURE 1.**

HIGHLIGHTS
➢ Unlocking the potential of CT scans: Role of medical images, CT applications, hazards,

The associate editor coordinating the review of this manuscript and approving it for publication was Humaira Nisar .
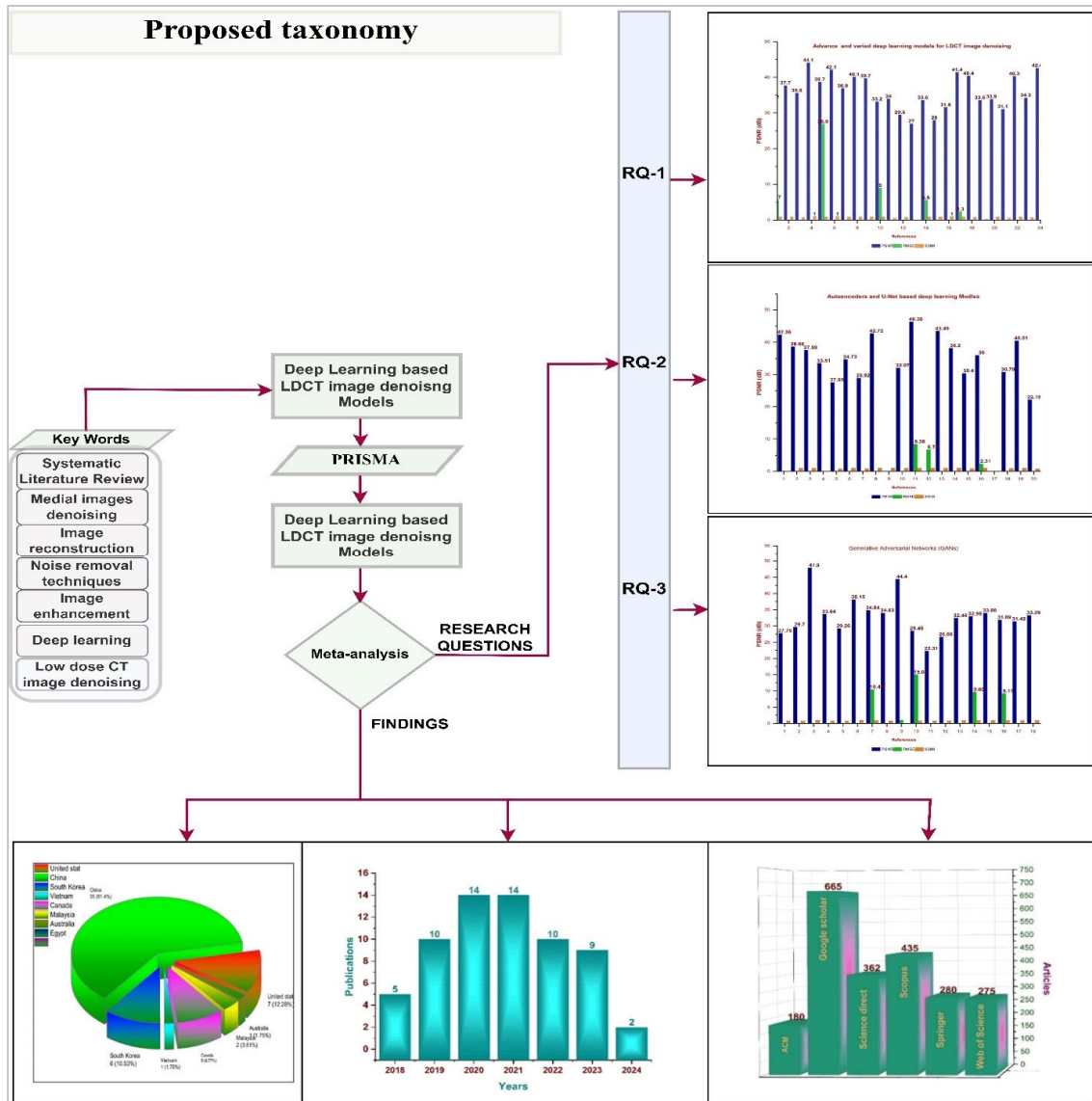
FIGURE 1. Graphical abstract.

- risk mitigation techniques and LDCT inception.
- ➢ Exploring LDCT image denoising: Traditional methods vs. deep learning models.
- ➢ Inside the CT scan: Understanding CT acquisition process, radiation absorption, noise types, and noise distribution patterns in LDCT images.
- ➢ Advancing LDCT image denoising: Crafting three research questions and navigating PRISMA selection.
- ➢ Charting the LDCT image denoising expedition: A comprehensive guide for new researchers, unveiling insights, discussion, and future endeavors.

I. INTRODUCTION

The advent of Artificial Intelligence (AI) and Deep Learning (DL) has made a substantial impact on various applications in medical image processing [1]. Medical imaging can rescue 40,000 lives annually, saving over 200 billion euros. Moreover, it can free up medical experts for 1.8 billion hours, i.e., equivalent to having an additional 500,000 full-time healthcare [2], [3]. In the realm of medicine, a variety of medical imaging modalities are used. However, CT scans provide a superior tissue distinction and the ability to gather detailed 3D information, overcoming the limitations of traditional X-ray procedures [4]. Additionally, a CT scan can simultaneously capture soft tissues and blood vessels to diagnose pathological abnormalities such as malignancies, vascular disorders, internal traumas, lung nodules, and bone fractures at the primary stage [5]. The CT scan has many contributions to medical treatment, but ionized radiation is one of the main pitfalls, especially for those with multiple CT scans. CT imaging relies on the radiation absorption characteristics of tissues, particularly their atomic number, to distinguish

between 'gray and white matter'. In a routine CT examination, one can receive a radiation dose of approximately 1.5 - 20 millisieverts (mSv), depending on the body tissue's sensitivity and the radiation absorption rate [6], [7]. Further, to enhance the internal visibility of veins, an iodinated contrast agent will be injected, doubling the radiation absorption rate of the human body during CT acquisition. Additionally, Shao et al. [7], added that in the case of CT radiation exposure, the risk of "*thyroid cancer*" is raised, with an odds ratio (OR) of 2.55 and a 95% confidence interval (CI) ranging from 2.36 to 2.75. Also, the risk of "*leukemia*" is increased, with an odds ratio (OR) of 1.55 and a 95% confidence interval (CI) ranging from 1.42 to 1.68. The risks of "*leukemia*" and "*thyroid*" cancer associated with CT scan exposure were greater in women than in males [8].

The CT imaging community employs the 'As Low As Reasonably Achievable' (ALARA) principle to minimize radiation exposure [9]. To limit the radiation dosage used in CT scans, Low Dose (CT) scanning technology was introduced. It employs two methods: The first way is to decrease the X-ray tube flux, while the second technique involves reducing the number of scan trajectories [6], [10]. In both cases, the signal-to-noise ratio (SNR) of X-ray signals is reduced, resulting in low-contrast CT images with noise, artifact, and visual impairment. These visual deteriorations blur feature edges, reduce organ and texture contrast, and compromise the reliability of clinical diagnostic procedures. Removing noise and artifacts from LDCT images while preserving critical features presents significant challenges [4], [11]. Various algorithms are used to enhance the LDCT image quality by reducing noise, eliminating artifacts, and improving visual clarity.

These algorithms are divided broadly into three major categories over the last five decades [12], i.e., 'Sinogram filtering techniques', 'Iterative reconstruction techniques', and 'Image domain processing' as given in **FIGURE 2**.
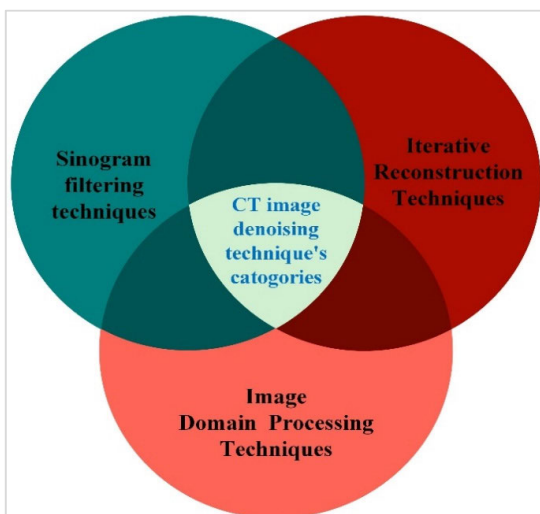
FIGURE 2. CT image denoising techniques.

The "*Sinogram filtering techniques*" work directly on the raw projection data generated before back-projection to precisely compute the noise statistics. It includes 'Bilateral filtering', 'Structural adaptive filtering', and 'Penalized weighted least squares algorithm' [13]. These techniques leverage a combination of physical and photon statistical characteristics to achieve effective denoising of CT images. However, it faces challenges such as edge blurring, low contrast, and dependence on vendor-specific projection data, which is not publicly available [14]. Further, the "*Iterative Reconstruction Technique*" depends on the image's prior information and is used to remove the noise and artifacts from the LDCT image by iterating between the sinogram and image domain. The iterative reconstruction-based restoration techniques include 'low-rank approximation', 'total variation', 'Dictionary learning', and 'non-local means' [15]. These methods help to enhance the quality of images during the restoration process. However high computational costs and content loss limit their denoising effectiveness [1], [16]. The "*Image Domain Processing Techniques*" are used to remove the noise and artifacts directly from the reconstructed image, independent of the projection data. Furthermore, LDCT image-denoising techniques are divided into two main categories: traditional CT image-denoising techniques and deep learning methods. Where, the conventional techniques typically establish a straightforward connection between relevant information and CT image noise, and then optimization algorithms are used to acquire denoised LDCT images. Such methods usually rely on prior knowledge about noise. Some popular traditional CT image denoising approaches include 'Wavelet base denoising' methods. It effectively improves the CT image quality by filtering out small coefficients associated with noise, however, these methods introduce some degree of blurring or loss of fine details in the image [17], [18]. Also, 'BM3D filtering' enables clearer and more accurate visualization of anatomical structures, though BM3D filtering was unable to remove streaking artifacts near bones [19]. Further, 'Dictionary learning' intuitively interprets and removes Gaussian noise from natural images but is limited effective in handling the complex noise model found in LDCT images. Furthermore, 'Non-Local Means (NLM)' algorithms are successfully denoise the CT images and preserve the features, however, it has a high computational complexity, which can result in lengthier processing times, especially for large images or high levels of noise. [20].

The traditional CT image denoising techniques are computationally expensive and may produce artifacts in flat regions as noise levels rise. Consequently, deep learning-based methods have emerged as a promising solution, and there is growing interest in leveraging these methods to improve the quality of LDCT images. Numerous review papers [1], [2], [3], [4], [5], [6], [8], [9], [10], [11], [12], [13], [18] have delved into deep learning denoising techniques, revealing their promising potential. However, a critical gap in the literature exists, necessitating a comprehensive review of state-of-the-art deep learning-based denoising techniques in

LDCT imaging. Such a review should not only assess existing methodologies, their strengths, and weaknesses but also visually present the performance of these algorithms, based on metrics. Furthermore, analyzing the current gaps in the literature regarding the assessment of CT image acquisition within clinical contexts involves examining the nuanced variations in radiation absorption across different anatomical regions, as well as discerning the origins and distribution of noise within the LDCT images.

The main contribution of this paper is given below.

I. Explore the roles of medical images, CT applications, hazards, and risk mitigation, as well as LDCT inception. Then, compare traditional vs. deep learning LDCT image denoising methods.

II. Evaluate CT image acquisition in the clinic, examining how radiation is absorbed in different parts of the body and identifying sources of noise and its distribution in the LDCT imaging data.

III. Investigate advanced and varied models such as CNNs and its variants, Transformer, Diffusion, Encoder-decoder, U-Net, and Generative Adversarial Network (GAN) for deep learning-based LDCT image denoising approaches followed by the ''PRISMA'', detailing the methodologies, and outlining the associated advantages and disadvantages of these algorithms.

IV. Assessing these methodologies involves scrutinizing diverse metrics, each with quantifiable values based on their dataset. This meticulous examination not only gauges the efficacy of these approaches but also serves as a comprehensive guide for newcomers, simplifying the identification of multidisciplinary research prospects. Leveraging dataset information, newcomers can readily discern the adequacy and relevance of datasets, aiding in their decision-making process for research initiatives.

V. Report on the primary contributors to LDCT image denoising, including key authors, prominent keywords, author connectivity, algorithms described in the literature, and the most reliable dataset for evaluating the model's performance.

VI. Discusses future research directions, identifying knowledge gaps in a subject area emphasizes their existence and enables experienced professionals to promote a more objective understanding of the field.

The rest of this paper is structured as follows: Section II provides an overview of CT images, covering its acquisition process, sources of noise, and methods for simulating noise in normal CT images. Section III explores methods, i.e., further divided into three sub-sections: Planning, Conducting, and Reporting, which covers the developed research questions, keywords, inclusion and exclusion criteria and standard procedures of PRISMA. Section IV critically analyses and discusses the findings of the review and contextualizes them within the broader literature. Section V delves into the existing research landscape, highlighting potential avenues of discussion and arguing the future research directions. Section VI presents the conclusion, critically evaluating recent LDCT image-denoising models, summarizing key findings, and highlighting their scientific impact in the field.

II. INSIDE CT SCAN
A. CT SCAN CLINICAL ACQUISITION PROCESS
In Computed Tomography, the word 'Computed' means calculated or reconstructed, while 'Tomography' is the combination of two words from Greek, i.e., 'Tomo' means cut or section, and 'graphy' means describe. So, a CT scan is an advanced computerized technology that collects data and converts it into cuts or cross-sectional slices of the human body. The X-ray tube and detector are typically mounted on the same rotating gantry normally in fourth-generation CT scan machines. They rotate around the patient in 360^0, a predetermined geometric alignment, emitting a beam of X-rays as given in **FIGURE 3**.
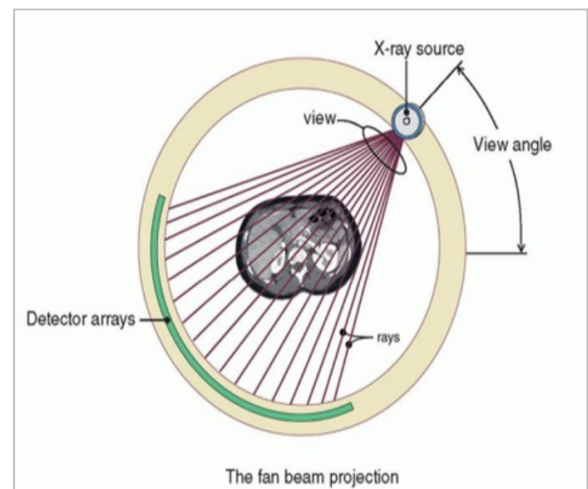
FIGURE 3. CT acquisition process in clinic.

The X-ray beam is passed through a patient body and received by the detector exactly opposite to the X-ray's source. The commonly used detector in CT imaging is called a 'Solid-state detector' or 'scintillation detector'. These detectors work by using crystals that light up when hit by X-ray photons, turning them into visible light. This light is then converted into electrical signals using photodiodes. Further processing includes amplification, filtering, and digitization to produce digital image data. The normal energy used in general CT scans falls within the range of 100-150 kV [6], [7]. The absorption of X-rays in the human body primarily depends on the atomic number and density of tissues encountered [6], [7]. **Table 1** reflects the different body parts and the relevant radiation absorption rate.

In CT imaging, contrast media is frequently utilized to highlight features which might not be easily observed. 'Oral contrast' is useful to scan the digestive tract, while 'intravenous contrast' is utilized to highlight organs and show blood arteries [7]. During a CT scan, a 'colorless iodine

TABLE 1. Body parts and radiation.

Body Parts	Radiation absorbed (mSv)
Head CT	1–2
Chest CT	5–7
Abdomen CT	5–7
Abdomen and pelvis CT	8–14
Coronary CT angiography	5–15
Coronary calcium CT	1–3

substance' that is impenetrable to X-rays is usually injected into a vein. The injection rate is typically 2-3 milliliters per second, resulting in a total volume of 100-150 milliliters. In the case of the contrast agent, the X-rays absorbed by the human body are double [7], [21], [22].

B. SOURCE OF NOISE IN CT IMAGES

CT scan is extremely sensitive to high contrast used to distinguish various soft tissues in the human body. However, this fundamental feature is vulnerable to the negative impacts of noise, particularly in the viewing of structures with low contrast. To effectively address image denoising, it is critical to have a complete grasp of the types of source noise and the overall properties of noise present in CT scans [23].

1) RANDOM NOISE

In LDCT, a deliberate reduction in the number of X-ray photons is employed to mitigate the risk of metabolic disorders. However, the finite number of photons detected during projection generates unpredictable fluctuation in image density, affecting the overall clarity and precision of the acquired CT data, such type of noise is called Random noise [8]. Random noise limits the ability of the radiologist to differentiate between two regions having different densities.

2) STATISTICAL NOISE

X-rays transmit energy in discrete packets known as quanta. The finite number of X-ray quanta is detected by the X-ray detector, and the detected count may vary due to statistical fluctuations. This variability, termed statistical noise or quantum noise, arises from the inherent uncertainty in detecting a finite number of X-ray quanta during each measurement [24].

3) ELECTRONIC NOISE

The detector receives photons that contain useful information about the interior structure of the human body. Electronic noise is caused by analogue electronic circuits that transform analogue signals into digital signals.

4) ROUND-OFF ERROR

Analog signals in CT scans are converted to digital signals through analog electronics before being reassigned to a computer for image reconstruction. Digital computers use

circuits to manage these discrete signals. However, the limited number of bits available for storing creates Round-off errors in mathematical computations, causing issues due to the need to represent amounts precisely. Round-off errors occur during the display stage of a CT image because CT scans only show a limited number of brightness levels. For example, if a unit only has 32 brightness levels, the difference between them is approximately 0.05 optical density units on the radiography film. However, the human eye can usually perceive much smaller variations (less than 0.004 OD). This constraint, especially in large display windows (100 or more CT units), might make it difficult for an observer to accurately interpret [25]. A brief visualization of these noise types in CT images is given in **FIGURE 4**.
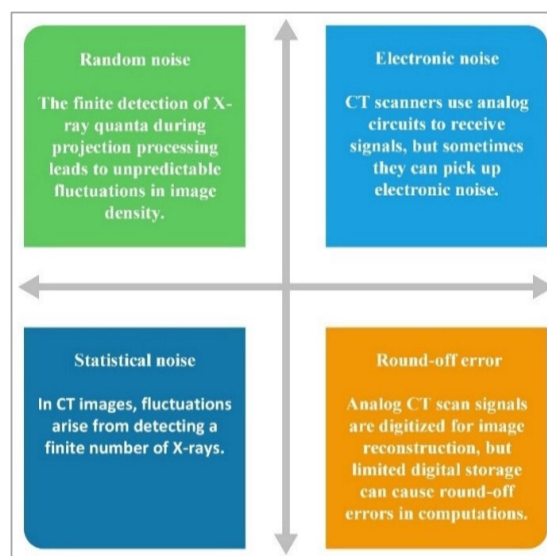
FIGURE 4. Noise sources in CT images.

C. NOISE DISTRIBUTION IN CT IMAGES

CT image noise is primarily introduced by electrical noise, round-off error, and random variations in detected X-ray intensity. CT numbers, defined by Hounsfield units (HU), represent tissue properties, and their accuracy depends on linearity in assigning the correct HU to a given tissue. Quantifying noise involves measuring fluctuations in CT numbers within regions of interest (ROIs), where Standard Deviation (SD) is a key indicator. Higher SD values imply more noise. Increased X-ray dose decreases quantum noise at detector elements. The noise distribution in CT images can be accurately characterized using the 'Poisson distribution', but for multi-detector CT scanners, the 'Gaussian distribution' is more suitable. Literature sources confirm that CT image noise generally follows an 'Poisson and Gaussian noise' pattern [3], [8], [26].

III. METHODS

This SLR examines recent research on deep learning-based techniques for LDCT image denoising. The literature selected for this review is followed by PRISMA guidelines [27],

No.	Research Questions	Description
RQ-1	What are advanced deep learning-based LDCT image-denoising models, and what are their advantages and disadvantages?	The main objective of this research question is to provide an in-depth exploration of the advanced and varied deep-learning approaches regarding LDCT image denoising, including CNNs and their variants, Transformer, and diffusion models. This inquiry aims to thoroughly investigate the methodology, potential effectiveness, advantages, and drawbacks of these approaches.
RQ-2	What are Encoder-decoder, and U-Net based deep learning LDCT image-denoising models, and what are their advantages and disadvantages?	This research question explores the use of Encoder-decoder and U-Net-based models for LDCT image denoising, with a focus on thoroughly analyzing their methodologies, benefits, and drawbacks. Additionally, it aims to evaluate their performance based on metrics such as PSNR, SSIM, and RMSE.
RQ-3	What are Generative Adversarial Networks (GANs) based LDCT image-denoising models, and what are their advantages and disadvantages?	This research question investigates the effectiveness of using GANs for denoising LDCT images. Additionally, various methodologies are assessed to understand their strengths and weaknesses, with performance metrics such as PSNR, SSIM, and RMSE evaluated on a specific dataset.

[28]. This SLR includes the 'Planning', 'Conducting', and 'Reporting' phases. Where, Planning involves recognizing the need, formulating research questions, and creating the review protocol. Conducting includes Literature Search, Study Selection, and Data Extraction & Synthesis. Reporting focuses on producing an unbiased review report summarizing the findings.

A. PLANNING

The planning phase of this SLR comprises several sub-phases. The first sub-phase involves recognizing the necessity for conducting an SLR, followed by formulating research questions and assessing the review protocol. This phase ensures that the SLR is systematically, and rigorously executed, and the research questions are clearly defined to guide the literature search process. Additionally, the planning phase aims to establish inclusion and exclusion criteria for selecting relevant studies. This process helps to minimize bias and enhance the comprehensiveness of the review.

1) IDENTIFY THE NEED FOR SLR

The current body of literature concerning LDCT image denoising exhibits notable deficiencies in several key areas. Firstly, there is a dearth of comprehensive exploration regarding the roles of medical imaging, especially CT scan, risks and risk mitigation strategies, and the inception of LDCT images. Furthermore, exploring CT image acquisition in clinical settings involves assessing how radiation affects various body parts differently. Moreover, identifying the sources of noise and its distribution in LDCT images reveals a significant gap in current research. Additionally, the evaluation of the latest deep learning models for LDCT image denoising including CNN, Transformer, Diffusion, Encoder-decoder, U-Net, and GAN-based algorithms along with their methodologies, advantages, and disadvantages. Lastly, there is a notable lack of discourse surrounding future research directions and knowledge gaps, which limits the advancement of LDCT image denoising research within the professional community. By conducting a state-of-the-art SLR in this area, we aim to bridge these gaps in knowledge and provide valuable insights for researchers, clinicians, and policymakers involved in LDCT imaging. This SLR will not only comprehensively analyze existing LDCT image denoising algorithms but also delve into the CT clinical equation process, radiation effects, noise sources and distributions.

2) IDENTIFY THE RESEARCH QUESTIONS

Research questions for this SLR are given in Table 2.

3) DEVELOPED AND EVALUATED THE REVIEW PROTOCOL

The protocol meticulously outlines methods, criteria, and procedures for the review process, ensuring systematicity, transparency, and reproducibility. Through rigorous evaluation, including feedback and revisions, the protocol is refined to enhance quality and suitability. Once finalized, it serves as a guiding framework for the review process, facilitating consistency and accuracy in the assessment of deep learning literature, thus ensuring reliable findings.

B. CONDUCTING

In the second phase, an extensive database search was conducted using predefined keywords to identify the most relevant articles. This section details the search strategy employed, the criteria for study selection, the process of data extraction, and the methods utilized for data synthesis. The search procedure involves the selection of appropriate source databases, defining the keywords, conducting the pilot search, refining the search keywords, and retrieving the primary studies from the source databases. The literature search strategy was divided into three sub-processes, as explained below.

1) LITERATURE SEARCH
a: SOURCE SELECTION

A selection of widely used digital libraries, scientific search engines, and databases were chosen to identify relevant articles for this SLR. These sources include Scopus, Google Scholar, Science Direct, Springer, Web of Science, and the Association for Computing Machinery (ACM).

b: SEARCH STRATEGY

To conduct a literature search relevant to the research questions, it is essential to identify and define appropriate keywords. The keywords have been defined and organized in Table 3. These criteria form the basis for searching through various electronic databases to select relevant literature.

TABLE 3. Keywords.

No.	Keywords and combination
1	("Low dose CT ") AND ("image denoising") AND ("deep learning" OR " Techniques" OR "algorithm" OR" methods")
2	"Low dose CT "AND ("image denoising" OR "image enhancement") AND ("deep learning" OR " Techniques" OR "algorithm" OR" methods")
3	("Low dose CT ") AND ("image Edge preserve denoising" OR "image enhancement" OR "Image Reconstruction") AND ("deep learning")
4	("Low dose CT ") AND ("image Edge preserve denoising" OR "Image enhancement ") AND ("deep learning "OR" Techniques" OR "algorithm" OR" methods")
5	("low dose CT ") AND ("Noise removal techniques" OR "LDCT denoising" OR "Image enhancement ") AND ("deep learning" OR" Techniques" OR "algorithm" OR" methods")
6	("Low dose CT ") AND ("Noise removal techniques" OR "LDCT denoising" OR "Image enhancement ") AND ("deep learning" OR "Neural network "OR" Techniques" OR "algorithm" OR" methods")
7	("Low dose CT image ") AND ("Noise removal techniques" OR "denoising" OR "enhancement "OR "reconstruction") AND ("deep learning" OR "Neural network. ")

Further, the search strategy is divided into two phases: the *primary* and *secondary* search. The primary search aims to identify potentially relevant studies comprehensively, from various online databases based on the defined keywords. While in the *Secondary* Search phase, a snowballing technique was used to find additional relevant studies. Forward snowballing involved checking references of selected articles, while backwards snowballing looked at bibliographies. This iterative process continued until we compiled a comprehensive list of relevant literature.

c: DATE AND TIME FRAME

The literature search spanned from January 2018 to 2024, employing predefined keywords and chosen search engines.

d: SEARCH FINDINGS

The initial comprehensive search retrieved a total of 2,197 articles from different databases including 665 articles retrieved from Google Scholar, 435 from Scopus, 362 from Science Direct, 180 from Springer, 275 from Web of Science, and 280 from the ACM library.

2) STUDIES SELECTION

After gathering all relevant publications, the filtering phase is critical to ensure the quality of the SLR.

a: INITIAL SCREENING

Two independent reviewers conducted an initial assessment of titles and abstracts retrieved from the literature search to determine their relevance to the research questions. Studies identified as potentially relevant by either reviewer underwent full-text screening. Further, inclusion and exclusion criteria serve as essential tools for reviewers to systematically identify and evaluate relevant studies, leading to more rigorous and informative research syntheses. Articles that meet the inclusion criteria specified in Table 4 are selected for full-text screening, while all those articles failing to meet the exclusion criteria specified in Table 5 are excluded.

TABLE 4. Inclusion criteria.

No.	Description
1	Articles should fall within the publication period from 2018 to 2024.
2	Articles must originate from reputable conferences, journals, thesis, or books.
3	The studies should focus on LDCT or medical image denoising using Deep Learning techniques.
4	The articles should focus on advanced deep learning models to denoise the LDCT images.
5	The article must be peer-reviewed.

TABLE 5. Exclusion criteria.

No.	Description
1	Articles that didn't focus on LDCT or medical image denoising will be excluded.
2	Articles that focused on public image denoising using DL models were excluded.
3	Articles that were not published in the English language were excluded.
4	Articles that utilized other image-denoising methods that did not use DL were excluded.
5	Articles published before 2018 were excluded.

TABLE 6. Table quality assessment rules (QAR).

No.	Description
1	Is the study focused on LDCT or medical image denoising or enhancement?
2	Is the study based on advanced deep learning models to denoise the LDCT images?
3	Are the aims and objectives of the defined DL model clearly articulated?
4	Are the DL models thoroughly explained?
5	Are appropriate metrics used to measure the performance of the DL model?

b: FULL TEXT SCREENING

After completing the initial screening of titles and abstracts, the next step involves obtaining the full text of selected articles. Two independent reviewers then meticulously examine each full-text article, evaluating it against the predetermined inclusion and exclusion criteria. Through this detailed assessment, articles that do not meet the specified inclusion criteria are identified and excluded. The reviewers carefully document the reasons for excluding each article during the full text screening process, ensuring transparency and reproducibility in the review. This documentation serves to provide a clear rationale for the exclusion of articles and facilitates a thorough understanding of the article selection process.
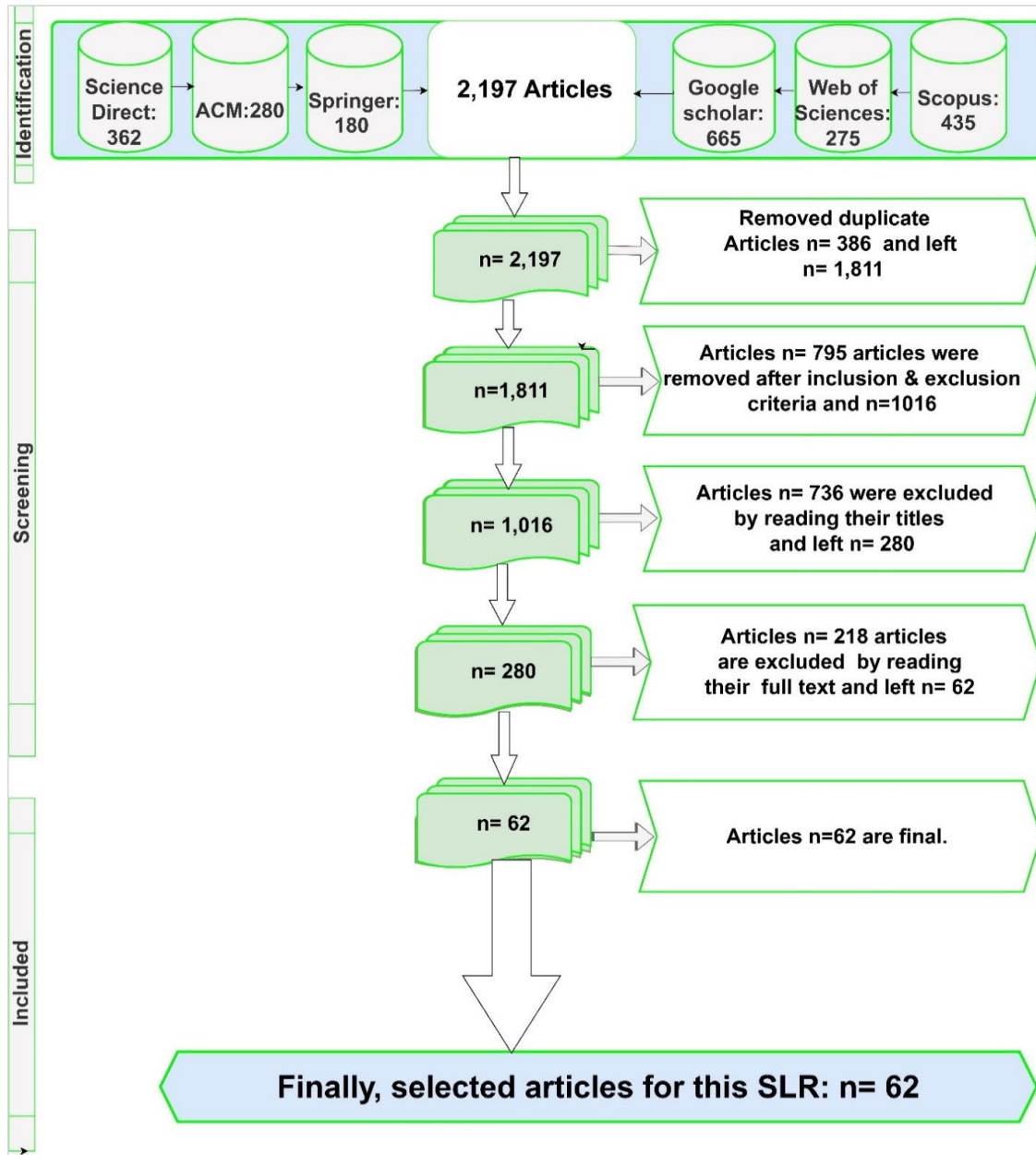
FIGURE 5. PRISMA flowchart: Review process overview.

c: QUALITY ASSESSMENT

Quality Assessment Rules (QAR) encompass a set of predefined criteria employed to assess the quality and relevance of the studies in this SLR. The objective of using QAR is to guarantee the inclusion of only high-quality studies, ensuring trustworthy and reliable results. By utilizing QAR, potential biases are minimized, and the transparency and reproducibility of the SLR process are enhanced. Also, Table 6 presents the fundamental principles of QAR used to select the most relevant articles for this SLR.

Based on the search and selection criteria total of 2,197 articles were selected from different search engines, where 386 duplicate articles were identified and removed, leaving 1,811 unique articles. After additional refinement, the pre-

defined inclusion and exclusion criteria led to the removal of 795 articles and leaving 1016 articles for further consideration. Subsequently, based on an assessment of their titles and abstracts, 736 articles were excluded, resulting in 280 articles remaining. After a thorough evaluation of the full texts, an additional 218 articles were excluded, resulting in a final set of 62 articles eligible for analysis and synthesis.

d: FINAL REVIEW AND CONSENSUS

All decisions made during the article selection process are carefully evaluated to guarantee consistency and correctness. Any remaining contradictions or doubts are addressed through discussion among the review team members. Finally, a consensus is achieved over the final list of included studies

for analysis and synthesis. The PRISMA diagram is a tool used in systematic reviews and meta-analyses to illustrate the flow of information through the different phases of the review process. The entirety of the review process is depicted in the PRISMA diagram **FIGURE 5**.

3) DATA EXTRACTION AND SYNTHESIS

During the data extraction and synthesis phase, relevant information from the selected studies is extracted based on the research questions. This phase involves populating a metadata table with the extracted data.

a: EXTRACTION OF DATA

The extracted data in this SLR pertains to the research questions, encompassing article references, methodologies, advantages, and disadvantages. Additionally, information about quantitative performance metrics such as Peak signal-to-noise ratio (PSNR), Structural Similarity Index (SSIM), and Root Mean Square Error (RMSE) are extracted based on the dataset used in the article to evaluate the efficacy of each study.

b: SYNTHESIZING OF DATA

This SLR, consisting of 62 articles, findings are meticulously analyzed, results are evaluated, trends are identified, and conclusions are drawn to effectively address the research questions.

c: DATA VALIDATION

In the data validation phase, the first author performed the initial data extraction, followed by the second author's thorough review and verification. Any discrepancies or concerns were carefully addressed and resolved through discussion and comparison of outcomes. This rigorous process ensured the accuracy and reliability of the extracted data. The resulting data were then summarized using a well-defined set of property values.

C. REPORTS

The data extracted from the 62 articles is systematically analyzed to address the three research questions. The findings corresponding to these research questions are succinctly presented across Table 8 through Table 13, which forming the basis for conclusions. Additionally, the current researcher's accomplishments are evaluated to provide insights for future research directions.

1) FINDINGS

In this SLR, a total of 62 studies were included. These studies were selected based on their relevance to the research questions addressed in the review. Specifically, out of the 62 studies, 21 studies were utilized to address RQ-1. Similarly, 21 studies were identified to support RQ-2. Furthermore, 20 articles were dedicated to addressing RQ-3. Table 7 summarizes the distribution of articles across the research questions.

TABLE 7. Articles and RQ.

RQ	Number of publications
1	21 (K1-K21)
2	21 (K22-K42)
3	20 (K43-K62)

FIGURE 6 visually illustrates the impact of different countries based on the number of articles and their corresponding publications. The data analysis reveals a noteworthy contribution from China, with 35 publications focused on LDCT image denoising using DL methods. This accounts for 61.4% of the articles in this SLR, highlighting China's dominant role and significant influence in advancing research within this specific domain. Prominently, the United States, South Korea, and Canada emerge as significant contributors, underscoring their active involvement and substantial contributions to this field of study.
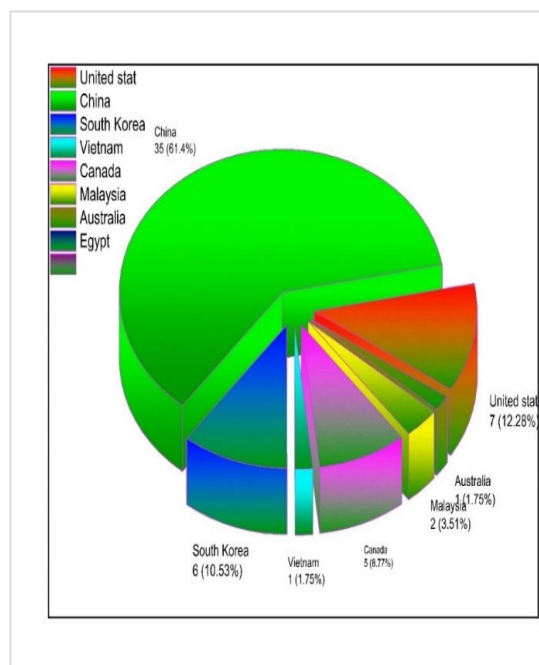
FIGURE 6. Relevant countries and publication counts.

The number of articles included in this SLR published (2018-2024) is shown in **FIGURE 7**. If the graph of the publications is carefully evaluated year-wise, it shows that this domain is a current trend and is an active research topic in the preceding five years. Furthermore, according to this SLR, 2020 and 2021 are the years with the most publications linked to LDCT image denoising based on DL, followed by, 2022.

FIGURE 8 illustrates the number of publications and sources before applying the inclusion and exclusion criteria. Six search engines are used to find related literature using keywords. Moreover, the figure reflects that Google Scholar is the primary source of article findings for this SLR, followed by Scopus and Science Direct.
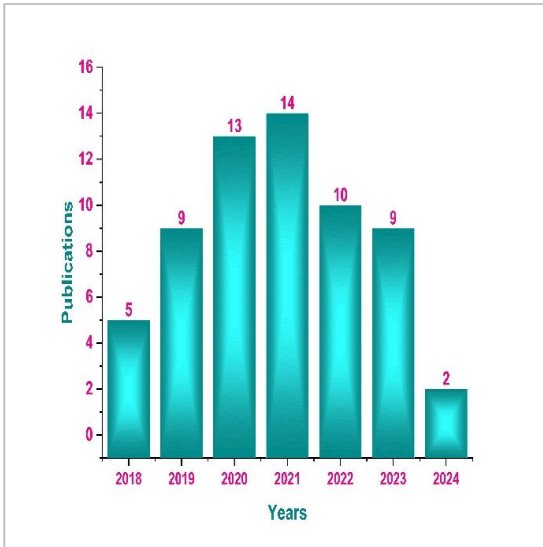
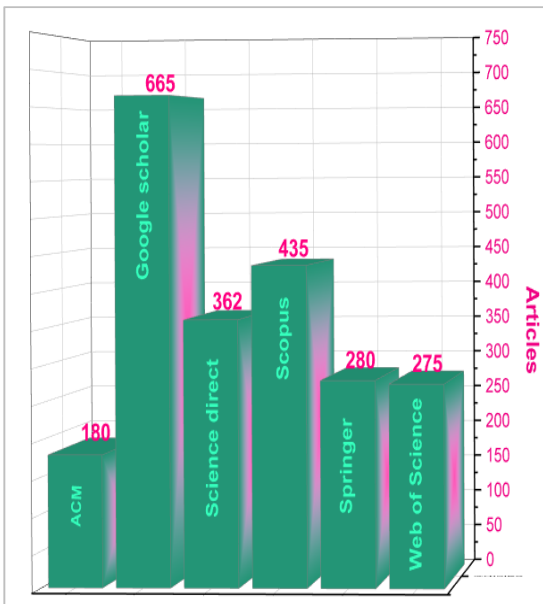**FIGURE 7.** Number of papers selected for review year-wise distribution.

FIGURE 9. Frequency of publication in selected journals and conferences.

FIGURE 8. Search engine-wise publications distribution.

FIGURE 9 offers valuable insights into the distribution of papers across journals and conferences, aiding in the identification of key sources of research within the topic area and providing context for the findings of this SLR. The graph illustrates that the IEEE Transactions journal stands out as the primary source for articles selected in this review, followed by IEEE conferences and then IEEE Access.

2) RESEARCH QUESTIONS

a: RQ-1: WHAT IS ADVANCED DEEP LEARNING-BASED LDCT IMAGE-DENOISING MODELS, AND WHAT ARE THEIR ADVANTAGES AND DISADVANTAGES?

This section provides a comprehensive exploration of advanced deep-learning approaches for LDCT image denoising, encompassing CNNs and their variations, Transformer
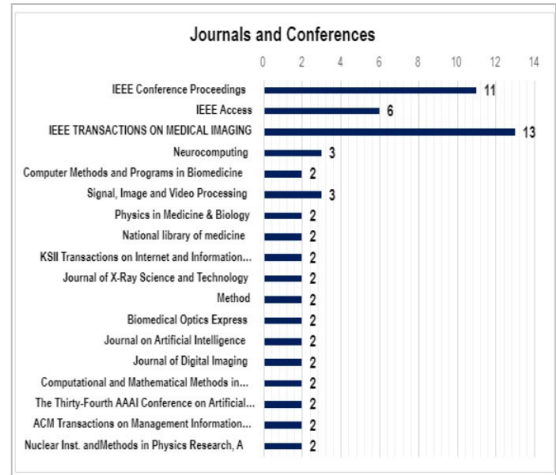
models, and diffusion models. Medical imaging, particularly CT, plays a pivotal role in diagnosis and treatment planning. However, the inherent noise in LDCT images poses a significant challenge, necessitating advanced denoising techniques for improved diagnostic accuracy. CNNs play a critical role in LDCT image denoising by extracting relevant features, capturing complex relationships, and mapping noisy input images to cleaner output images. However, CNN-based methods are restricted by their receptive field, which limits their capability to capture contextual information with long-range spatial dependencies across feature maps [29]. Further, Transformer is a deep learning architecture originally introduced for Natural Language Processing (NLP) tasks by Vaswani et al. in 2017. The core idea behind the Transformer architecture is self-attention mechanism, which allows the model to weigh the importance of different elements in the input sequence. Transformer-based approach for LDCT image denoising leverages the self-attention mechanism to capture global dependencies and effectively remove noise and artifacts while preserving important structural information in the images, but The transformer-based method lacks precision in capturing fine details, potentially leading to denoised images that could impact a physician's assessment of lesion conditions [29], [30]. Furthermore, diffusion models are deep generative models, based on two stages: forward diffusion and reverse diffusion. During the forward diffusion phase, Gaussian noise is incrementally added to the input CT image data across multiple iterative steps.

This process simulates the gradual propagation of noise within the image. In contrast, the reverse diffusion phase involves training a model to systematically undo the diffusion process, aiming to accurately reconstruct the original noise-free CT image data. However, diffusion models are computationally expensive and slow as involve several steps [31]. This comprehensive review explores and evaluates various denoising methods presented in recent studies, analyzing their methodologies, advantages, and disadvantages as given in Table 8. It aids practitioners and researchers in

TABLE 8. Exploring advanced deep learning based denoising techniques.

References	Methodology	Keys
	Advantages	
	Disadvantages	
Shan et al. [32]	The study employed a Modularized Adaptive Processing Neural Network (MAP-NN) trained on LDCT data, which was then compared to commercial reconstruction.	K1
	The deep learning approaches given a batter performance compared to the IR techniques.	
	The proposed network is not customized to a particular vendor or entity.	
Ming et al. [33]	This paper proposed dense connections, residual learning, and batch normalization layers.	K2
	The proposed network demonstrated a 7% reduction in RMSE compared to other state-of-the-art denoising methods in the literature.	
	The proposed network requires more time to train.	
Gou et al. [34]	The GR-CNNs incorporate gradient information as a regularization term during network training to preserve edge information while removing CT image noise.	K3
	The proposed method performs image denoising and sharpening with excellent perceptual and statistical performance.	
	It requires many parameters, which may result in longer training times and increased computational complexity.	
Gholizadeh et al. [35]	The proposed method integrates dilated convolution, residual learning, edge detection, and perceptual loss to denoise CT images.	K4
	Improved denoising performance compared to existing methods in terms of both objective and subjective evaluations.	
	Requires longer training times compared to some existing methods.	
Kang et al. [36]	This paper uses a multi-stage Wavelet Residual Networks architecture to combine deep learning, and framelet transforms for image denoising.	K5
	Effectively mitigates streak artifacts commonly present in LDCT scans while preserving important organ texture features and retaining critical lesion information.	
	High computational complexity compared to traditional denoising methods.	
Liang et al. [37]	The paper presents a Densely Connected Network (DCN) with edge enhancement and a compound loss function.	K6
	The proposed denoising model outperforms the existing methods in the literature to preserve image details and suppress the noise.	
	The proposed EDCNN method must be revised in low denoising efficiency and over-smoothed results.	
Feng et al. [38]	The DRCNN utilizes two residual learning pathways to learn the mapping between low-dose and high-dose CT images.	K7
	The proposed DRCNN method reduces computational time.	
	The suggested network must reduce the computational costs associated with forward- and back-projections.	
Kim et al. [39]	This method trains the denoiser without relying on paired datasets of LDCT and NDCT scans of the same individual in similar environments.	K8
	Eliminates the need for paired datasets and improves denoising and qualitative and quantitative performance.	
	This method requires careful parameter tuning to achieve optimal performance, which may be time-consuming and computationally expensive.	
Zhang et al. [40]	This paper introduces Adaptive Global Context (AGC), an innovative method for denoising LDCT images. The AGC-LSRED network includes AGC attention and a compound loss function.	K9
	The proposed algorithm effectively reduced the noise.	
	The RMSE value has increased, while denoising shows an imbalanced result.	
Song et al. [41]	This article presented a cascaded multi-supervision convolutional neural network to minimize rician noise in MRI images and perfusion noise in CT images.	K10
	The proposed approach is robust in both specified noise level and blind noise level cases.	
	The suggested protocol's structure is complex, making it challenging to implement.	
Trung et al. [42]	This paper proposed a receptive field to capture more contextual information and introduced a two-stage denoising approach that combines both pixel-wise and patch-based denoising.	K11
	Effectively reduces noise in LDCT images while preserving more image details.	
	This technique requires a significant amount of time for training results in computationally expensive.	
Chen et al. [43]	This study presents LIT-Former, a novel approach for denoising 3D LDCT images. LIT-Former combines in-plane and through-plane transformers, incorporating efficient Multi-head Self-attention Modules (eMSM) and streamlined Convolutional Feed-forward Networks (CFN).	K12
	LIT-Former reduces computational complexity compared to 3D convolutional approaches while enabling rapid convergence.	
	Sparse availability of suitable datasets necessitates data simulation and may pose validation challenges in clinical settings.	
Huang et al. [44]	This methodology utilizes residual learning and multi-level feature fusion to improve the quality of the denoised images.	K13
	Improves the quality of LDCT images by simultaneously denoising textures and enhancing structures with high accuracy and efficiency.	
	This may result in t in a loss of image sharpness and the appearance of smoothness in some cases.	

TABLE 8. *(Continued.)* Exploring advanced deep learning based denoising techniques.

YOU et al. [45]	This paper uses skip connections and network-in-network blocks to extract features from the input LDCT image.	K14
	Preserves essential features and offers superior image quality.	
	It has a relatively long training time and high computational complexity.	
Chen et al. [46]	This paper introduced a residual CNN which uses residual blocks, skip connections and fractional TV loss regularization.	K15
	The proposed network removed noise and artifacts in LDCT images effectively.	
	Training takes more time and effort, and incorporating new data is challenging.	
Zhong et al. [47]	This paper presents transfer learning and residual networks, where the residual network is pre-trained on natural images using transfer learning and fine-tuned on a small dataset of low-dose CT images.	K16
	Preserved more texture details at a low computational cost and prevented overfitting.	
	This technique utilizes a small dataset of LDCT images for fine-tuning, which can be challenging to obtain in some cases.	
Yang et al. [48]	This paper presents a residual dense network with self-calibrated convolution, incorporating jump and dense connections to enhance feature utilization.	K17
	The proposed methodology can be trained using a small number of images to maintain sharp edges and tiny details.	
	The algorithm has a complicated architectural design.	
Gao et al. [49]	CoreDiff leverages LDCT images to displace noise and employs a mean-preserving degradation operator to mimic CT degradation, reducing sampling steps. Additionally, it proposes CLEAR-Net to alleviate error accumulation during restoration.	K18
	CoreDiff's approach significantly reduces inference time while maintaining flexibility and performance.	
	The proposed technique has a relatively slower inference time compared to RED-CNN-based and GAN-based models, despite being faster than DDM2 and IDDPM.	
Yan et al. [50]	This paper uses a convolutional dictionary learning with a compound loss to increase feature extraction and visual quality.	K19
	The proposed method conserves feature and shows adaptability for broader medical imaging applications.	
	The primary issue in medical imaging is the lack of paired training data and specific streak artifacts.	
Marcos et al. [51]	The paper presents a ResNet with fused attention modules and integrated loss functions for denoising LDCT images.	K20
	The proposed technique achieves textural features without over-smoothing.	
	The model has substantial computational expenses.	
Luthra et al.[52]	The proposed method, Eformer, combines CNN and transformer-based networks to extract features while preserving image details.	K21
	The proposed method effectively preserves image details by targeting image edges, resulting in superior denoising performance.	
	Limited training data diversity or poor quality may limit the Eformer method's applicability to other medical imaging tasks.	

informed decision-making for effective application in this field.

In Table 9 performance metrics such as PSNR, RMSE, and SSIM are utilized to evaluate the effectiveness of various advanced deep learning techniques applied in LDCT image denoising, as documented in various research papers within this SLR. Where, larger values of PSNR and SSIM indicate better performance, while smaller values of RMSE suggest better accuracy. It will help to analyze the effectiveness of different methods while improving the quality of LDCT images. By examining the results reported in each study, based on a specific dataset, researchers can assess the strengths and weaknesses of different techniques and potentially identify trends or areas for further investigation in the field of LDCT image processing.

FIGURE 10 indicates data showcasing PSNR, RMSE, and SSIM values for different LDCT image denoising techniques and datasets offer significant benefits for researchers in this field. Firstly, such visual representation facilitates the quick observation of performance trends across various denoising methods. Researchers can easily discern which techniques consistently achieve better results across multiple datasets and which metrics are most impacted by specific denoising techniques. For example, K16 have high PSNR values indicate better denoising performance in terms of preserving image quality. Also, higher RMSE i.e., K5 indicates larger differences between the actual CT image and ground truth image.

Further, the analysis of the graph can inform future research directions by pinpointing areas where current techniques may be lacking or where improvements are needed. For instance, if certain techniques consistently exhibit low SSIM values across multiple datasets, it indicates a need for further research to enhance their ability to preserve structural information. This guidance can lead to the development of novel algorithms aimed at addressing the unique challenges of LDCT image denoising. In essence, the graph serves as a valuable tool for researchers, offering insights into performance comparison, technique selection, and guiding advancements in LDCT image denoising research.

TABLE 9. Quantitative analysis of advanced deep learning based denoising models.

Reference	Datasets Used	PSNR	RMSE	SSIM
K2	The Cancer Imaging Archive (TCIA) dataset.	33.67	5.65	0.94
K3	AAPM Low-Dose CT Grand Challenge.	37.74	X	0.92
K4	Lung dataset Metric.	35.57	X	0.69
	Piglet dataset.	44.12	X	0.98
	TCIA dataset.	31.50	X	0.54
K5	2016 NIH AAPM-Mayo Clinic Low-Dose CT Grand Challenge.	38.71	26.9	0.89
K6		42.08	0.01	0.98
K7	Simulated Dataset.	36.94	0.03	0.93
K8	XCAT datasets.	40.11	X	0.94
	Mayo Clinic datasets.	39.65	X	0.93
K9	Simulated dataset.	32.75	6.04	0.98
K10	Clinical CT noisy image.	33.97	X	0.64
K11	AAPM Low Dose CT Grand Challenge dataset.	29.45	X	0.82
K12	2016 AAPM Grand Challenge dataset.	34.35	1.80	0.86
	Simulated dataset.	43.10	0.65	0.97
K13	2016 NIH-AAPM- Mayo Clinic Low Dose CT Grand Challenge.	33.60	5.58	0.88
K14		28.02	0.04	0.88
K15		31.59	0.03	0.93
K16	TCIA dataset.	41.44	2.31	0.98
K17	2016 NIH-AAPM- Mayo Clinic Low Dose CT Grand Challenge.	40.40	X	0.81
K18		43.92	0.97	12.9
K19		33.93	X	0.92
K20	Thoracic dataset.	31.07	X	0.64
	Abdomen dataset.	40.33	X	0.91
	Chest dataset.	34.26	X	0.69
	Chest head dataset.	42.64	X	0.687
	Piglet dataset.	40.93	X	0.98
K21	AAPM Low Dose CT Grand Challenge dataset.	43.49	0.1	0.99

Where *X denotes that the algorithm hasn't been assessed on that metric.

b: RQ-2: WHAT ARE ENCODER-DECODER, AND U-NET-BASED DEEP LEARNING LDCT IMAGE-DENOISING MODELS, AND WHAT ARE THEIR ADVANTAGES AND DISADVANTAGES?

In the realm of medical imaging, the demand for enhancing the quality of LDCT images has fueled the development of innovative denoising models such as Encoder-decoder and U-Net. In these models, the Encoder-decoder architecture compresses input LDCT scan images into a lower-dimensional representation known as latent space. In contrast, U-Net architectures incorporate skip connections between corresponding layers in the encoder and decoder, facilitating the preservation of spatial details during image reconstruction. These models, based on Encoder-decoder architectures, sparsity constraints, spectrum loss functions, and multi-dimensional spatial attention mechanisms, intend to learn low-dimensional feature representations efficiently while minimizing radiation exposure. These methods provide unique strategies for LDCT denoising, with ongoing technical advancements targeting further improvements in their performance for clinical applications. The methodologies, advantages, and disadvantages of the latest Encoder-decoder and U-Net models have been outlined in Table 10.

Table 11 reflects the performance of Encoder-decoder, and U-Net models exits in this SLR. Based on the met-rics provided, the evaluation of denoising models for LDCT images reveals distinct performance trends. Models exhibiting higher PSNR and SSIM values, alongside lower RMSE values, demonstrate superior noise reduction capabilities and greater fidelity to the original images. These metrics provide valuable insights into the efficacy of different denoising approaches, guiding the selection of models that best meet specific requirements for LDCT image enhancement.

Figure 11 visual illustration of the denoising algorithm's performance using PSNR, SSIM, and RMSE. Further, PSNR measures image fidelity, with higher values indicating better quality, SSIM evaluates structural similarity, where higher scores signify greater similarity, and RMSE quantifies prediction accuracy, with lower values indicating better performance. Visualizing the evaluation metrics in the form of a graph provides a concise and informative summary of different denoising algorithms, helping the researchers make informed decisions and advancements in LDCT images.

c: RQ-3: - WHAT ARE GENERATIVE ADVERSIAL NETWORKS (GANs) BASED LDCT IMAGE-DENOISING MODELS, AND WHAT ARE THEIR ADVANTAGES AND DISADVANTAGES?

GANs are deep learning models that consist of a generator and a discriminator. The generator generates synthetic data resembling real data, while the discriminator distin-
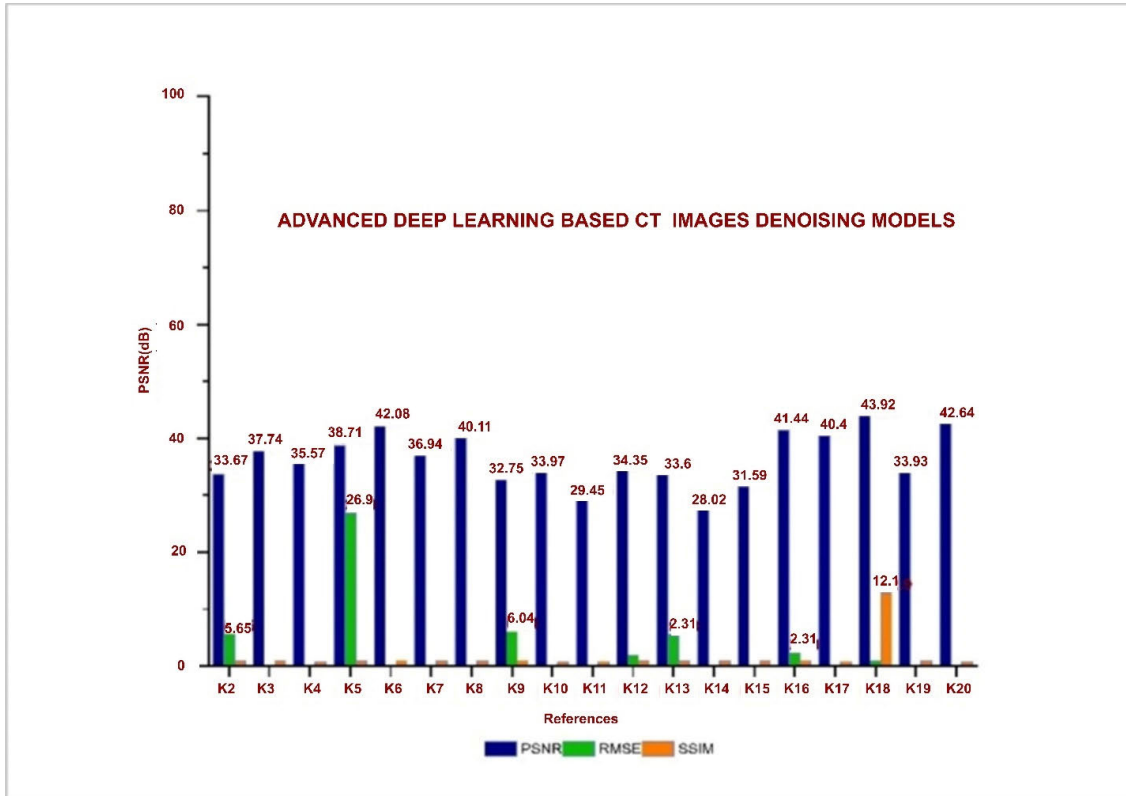
FIGURE 10. Advanced and varied deep learning model for LDCT image denoising.

guishes between real and synthetic samples. By training these networks, GANs improve the generator's ability to create realistic illustrations.

In LDCT image denoising, integrating generative and discriminative models in a hybrid learning approach using GANs has gained popularity. This approach employs different CNN architectures, such as Encoder-decoder, U-Net, and ResNet, to enhance LDCT image quality. Table 12 provides an insightful overview of the GANs models employed for LDCT image denoising. It presents the methodologies utilized by each model, accompanied by a comprehensive analysis of their respective advantages and disadvantages.

Table 13 presents an array of performance metrics evaluating the GANs algorithm across various datasets. Notably, the algorithm's effectiveness is assessed using PSNR, RMSE, and SSIM metrics. Datasets utilized for testing encompass a diverse range, including those from the Mayo Clinic, Lung's Grand Challenge, Piglet, and the 2016 NIH AAPM-Mayo Clinic Low-Dose CT Grand Challenge. These datasets offer a broad spectrum of imaging scenarios for evaluation. Results indicate a significant variability in the algorithm's performance across different datasets and metrics. PSNR values range widely from 22.31 to 47.90, reflecting differences in image quality and fidelity. Similarly, RMSE values fluctuate between 0.02 and 15.04, suggesting discrepancies in the accuracy of reconstructed images. Interestingly, SSIM values remain relatively consistent, hovering between 0.69 and 0.98, indicating a degree of stability in preserving structural infor-

mation across diverse datasets. The LDCT-DLR algorithm's performance can also be compared with established benchmarks, such as the 2016 NIH AAPM-Mayo Clinic Low-Dose CT Grand Challenge dataset, providing valuable insights into its efficacy relative to industry standards. However, further analysis and validation against larger and more diverse datasets are warranted to comprehensively assess its utility and reliability in clinical practice.

FIGURE 12 depicting performance metrics (PSNR, RMSE, SSIM) across datasets and algorithms offers quick insights for researchers. PSNR indicates image quality, RMSE signifies reconstruction accuracy, and SSIM reflects structural preservation. Researchers can identify top-performing algorithms and areas needing improvement, aiding in algorithm selection and optimization efforts.

d: BIBLIOGRAPHY VISUALIZATION
FIGURE 13 reflects the keywords used in the publications employed in this SLR.

Visualizing the related keywords enhances the accessibility, searchability, and visibility of related literature, thereby increasing its effectiveness in disseminating knowledge and fostering further research in this field, allowing the researchers to efficiently locate relevant publications by tracing connections between keywords. Furthermore, the diagram serves as a guide for further research by highlighting gaps or areas that have received less attention, prompting

TABLE 10. Methodologies of encoder-decoder and U-Net models.

References	Methodology / Advantages / Disadvantages	Keys
Liu et al. [53]	This paper used an Encoder-decoder with sparsity constraint to restore LDCT images, avoid additional radiation exposure, and efficiently learn low-dimensional feature representations for image analysis tasks.	K22
	The proposed approach achieves efficient learning of low-dimensional feature representations.	
	The model's overfitting to the training data hampers its ability to generalize well to new, unseen data, resulting in poor performance.	
Liu et al. [54]	This paper modifies the ResUnet architecture by incorporating a spectrum loss function to improve image quality while reducing radiation exposure.	K23
	Compared to other existing approaches, the proposed method demonstrates superior results in denoising LDCT images while effectively preserving critical information.	
	Utilizing an MSE-based cost function in this method can result in blurry images as it cannot preserve high-frequency details.	
Feng et al. [55]	This method incorporates residual connections, U-net architecture, and multi-dimensional spatial attention mechanisms to enhance the images' quality effectively.	K24
	The proposed model effectively maintained more structural features of the lung tissue.	
	The evaluation of pixel intensities using MSE as an objective function can result in image blurring.	
Feng et al. [56]	This article introduces a modified dual-domain U-net approach for denoising LDCT imaging by integrating the image and sinogram domains.	K25
	By integrating information from the image and sinogram domains, the proposed approach enables more effective and efficient denoising of LDCT imaging.	
	Further validation and testing are necessary to ensure the technique's reliability and suitability for widespread clinical use.	
Li et al. [57]	This article introduces a multistage convolutional neural network incorporating an Encoder-decoder perceptual loss network.	K26
	Potentially enable a more accurate and efficient diagnosis to plan the patient's treatment.	
	It may require more computational cost and longer training time than traditional image reconstruction methods.	
Zhang et al. [58]	This study proposes a denoising method for LDCT images using U-Net, multi-attention mechanisms, and an enhanced learning module.	K27
	The proposed denoising method effectively removes noise in LDCT images while preserving detailed features.	
	It may require a longer computational time due to the utilization of multiple attention modules and an enhanced learning module.	
Juneja et al. [59]	This method combines a bilateral median filter with an Encoder-decoder network to denoise CT images by learning the mapping between the noisy and denoised images	K28
	The proposed network outperforms existing methods, demonstrating superior performance	
	The proposed approach focuses solely on Gaussian noise removal in LDCT images, but it exhibits artifacts during the denoising process.	
Liu et al. [60]	This paper introduces ERA-WGAT, a technique comprised of an edge-enhanced residual Encoder-decoder and a window-based graph attention convolutional network.	K29
	It resulted in improved denoising performance while preserving features effectively.	
	However, the number of nodes in ERA-WGAT remains higher compared to CNN.	
Zubair et al. [61]	This paper presents hybrid dilated convolution in U-Net Encoder-decoder along the batch normalization layer	K30
	The proposed method captures the local and global information and feature edges.	
	The proposed method validation is required on real-world datasets.	
Fan et al. [62]	This paper introduces Quadratic Autoencoder (Q-AE), a deep neural network architecture that leverages a quadratic loss function to enhance denoising performance.	K31
	Capable of capturing complex statistical dependencies between image pixels by utilizing a quadratic loss function.	
	It requires a substantial amount of training data and computational resources.	
Ma et al. [63]	This paper employs a Convolutional Neural Network (CNN) to learn the mapping between low-dose and standard-dose CT images and incorporates a residual connection to preserve fine image details.	K32
	The proposed model reduces noise while effectively preserving critical image features and structures.	
	The model's effectiveness relies on the availability of much training data and significant computing power.	
Wang et al. [64]	This paper proposes a two-stage training process using a denoising Encoder-decoder for low-dose CT denoising. The first stage trains an Encoder-decoder on noisy CT images, while the second stage uses a masking technique to address noise in low-dose CT images.	K33
	The proposed model achieved dose reduction without compromising image quality.	
	Further validation and comparison with advanced denoising techniques are necessary to confirm the effectiveness and reliability of the proposed model.	
Zubair et al. [65]	In this study, the DoG-UNet+ model integrates an innovative layer known as the "Difference of Gaussians (DoG) Sharpening Layer" into the existing U-Net architecture.	K34
	The proposed model achieved some promising results in terms of PSNR, SSIM and RMSE.	
	The proposed model needs to be checked on a real dataset.	
Shafai et al. [66]	The paper proposes a deep learning-based approach using an Encoder-decoder for denoising medical images.	K35
	The technique diagnosed pneumonia with 98% accuracy.	
	The proposed method needs to reduce training time.	

TABLE 10. *(Continued.)* **Methodologies of encoder-decoder and U-Net models.**

Saravanan et al. [67]	The paper introduces a deep learning-based approach for medical image reconstruction, utilizing Encoder-decoder and deep Boltzmann machine training.	**K36**
	This method achieves higher accuracy and computational efficiency in training than existing methods.	
	The utilization of MSE as an objective function can lead to image blurring.	
Yang et al.[68]	The method involves data augmentation techniques, constructing a convolutional Encoder-decoder model, and trained on clean and noisy image pairs.	**K37**
	The method demonstrated excellent denoising performance while preserving image detail.	
	The incorporation of these methodologies increases the network depth, thereby leading to longer training times.	
Chi et al. [69]	The paper presents a framework that combines noise estimation and super-resolution networks to improve the quality of CT images in a unified approach.	**K38**
	The proposed approach significantly enhances the accuracy of noise estimation compared to conventional filter-based techniques.	
	Estimation error increases continuously as the noise intensity rises.	
Han et al. [70]	The proposed Framed U-Net model combines DCFNet, a deep convolutional encoder, and a framelet decoder within a U-Net architecture.	**K39**
	The novel architecture achieved improved denoising performance on sparse-view CT images.	
	The proposed model may perform poorly on images significantly different from the training data.	
Li et al. [71]	The SACNN architecture comprises a feature extractor and a denoising block with a self-attention mechanism to capture long-range dependencies.	**K40**
	The SACNN method achieves state-of-the-art performance in LDCT image denoising.	
	The SACNN model requires a large amount of training data and has a high computational cost during training and inference.	
Ramanathan et al. [72]	The study introduces a novel CT image reconstruction method based on a convolutional Encoder-decoder network and vector quantization.	**K41**
	The proposed method effectively reduces the noise while preserving image quality.	
	The network architecture is complex and needs more training time.	
Chai et al. [73]	The model incorporates frequent pattern mining and an adversarial-based denoising Encoder-decoder to tackle feature engineering and label correlation challenges.	**K42**
	Annotation effectively highlights object abnormalities, providing better insights.	
	It may require a large amount of labelled training data to achieve optimal performance.	

TABLE 11. **Encoder-decoder and U-Net models.**

Reference	Dataset Used	PSNR	RMSE	SSIM
K21	Simulated dataset	42.36	0.01	X
K22	AAPM Low-Dose CT Grand Challenge.	38.66	X	0.95
K23	Simulated dataset.	37.59	0.01	0.93
K24	Simulated dataset.	33.51	0.03	0.9
K25	AAPM Low-Dose CT Grand Challenge.	27.55	X	0.79
K26	TCIA dataset.	34.73	X	0.93
	AAPM Low-Dose CT Grand Challenge	28.92	X	0.86
K27	TCIA dataset.	30.01	9.91	X
K28	2016 NIH AAPM-Mayo Clinic Low-Dose CT Grand Challenge.	42.72	0.01	0.96
K29	"KiTS19" grand challenge dataset.	X	0.01	0.96
K30	Mayo Clinic datasets.	32.07	0.02	0.95
K31	Simulated dataset.	46.36	8.38	0.99
K32	2016 NIH AAPM-Mayo Clinic Low-Dose CT Grand Challenge.	X	6.74	0.96
K33	COVID-19 grayscale chest dataset.	38.2	0.01	0.98
K34	Chest CT dataset.	30.4	X	0.87
K36	2016 NIH AAPM-Mayo Clinic Low-Dose CT Grand Challenge.	36	2.31	0.98
K36	Simulated dataset.	38. 5	X	0. 93
K37	TCIA dataset.	30.79	X	0.88
K38	2016 NIH AAPM-Mayo Clinic Low-Dose CT Grand Challenge.	40.51	X	0.94
K39		22.18	X	0.78
K40	LoDoPaB-CT benchmark dataset.	43.75	X	0.96

Where *X denotes that the algorithm hasn't been assessed on that metric.

researchers to explore underexplored topics or develop new research questions. **FIGURE 14** visually presents the popular models that were reviewed in this SLR. The diagram provides insights into the prevailing trends and directions in LDCT image-denoising research. It highlights advanced deep learning techniques, including generative models, multi-attention mechanisms, adversarial networks, and self-calibrated convolutions. The clustering and proximity of specific models in the diagram indicate shared characteristics and similarities in their design or methodology.

FIGURE 15 visualizes the connectivity and relationships among author's papers in this SLR, enabling a better understanding of the research landscape and facilitating further exploration and analysis in the field.
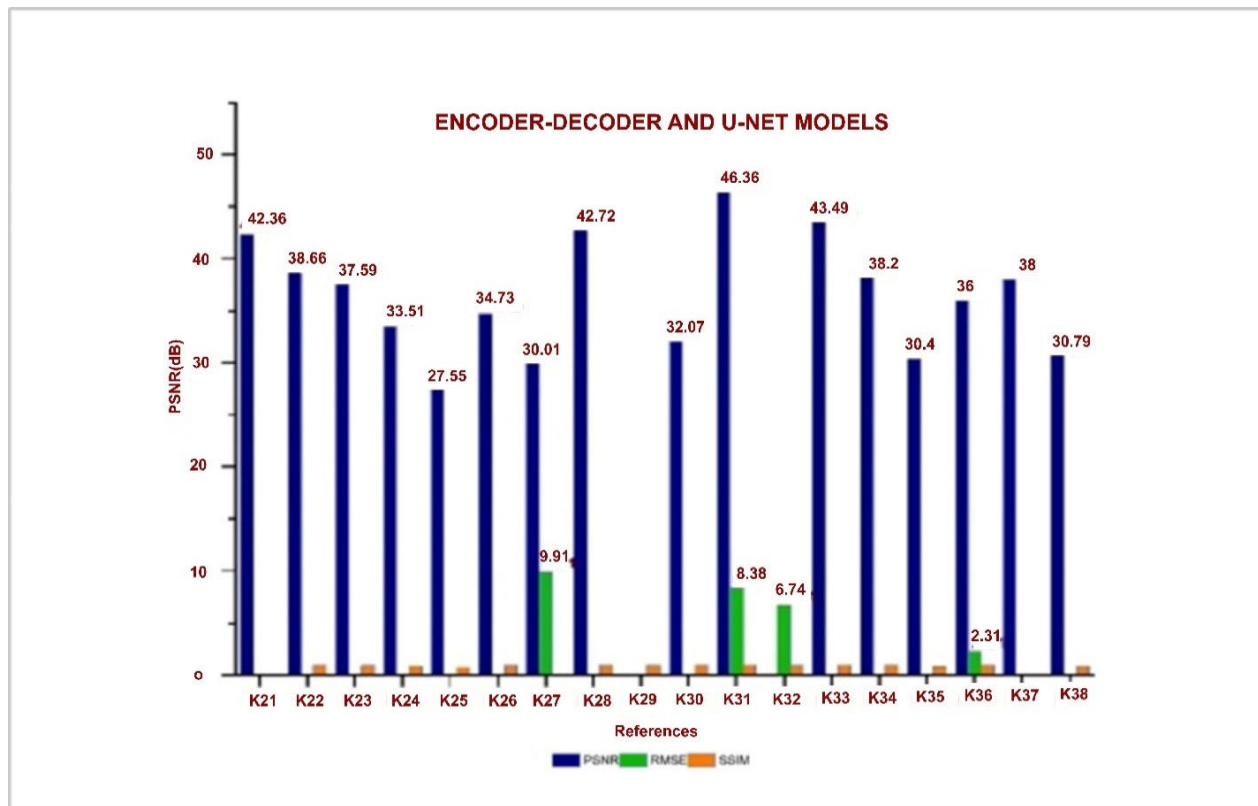
FIGURE 11. Encoder-decoder and U-Net models.

IV. DISCUSSION

This systematic literature review offers valuable insights into various aspects of medical imaging, with a particular focus on Computed Tomography (CT) applications and methods for denoising low-dose CT images. In contrast to the latest review paper [93], which focuses on the evolution of CNN techniques for CT image reconstruction, addressing challenges like computational complexity and exploring opportunities for decentralized and mobile imaging services. Further Lei et al. [94], evaluates deep learning methods for improving overall CT image quality by reducing noise and blurring using various CNN architectures like U-Net, V-Net, and ViT, along with different learning paradigms and evaluation metrics such as MSE, SSIM, and PSNR. Our proposed SLR takes a distinct focus on denoising LDCT images using advanced deep learning models. While these previous reviews may cover a broader range of topics or focus on different aspects of CT imaging. This review delves into the role of medical imaging and the risks posed by conventional CT scans, emphasizing the necessity of implementing risk mitigation strategies.

These strategies involve reducing radiation exposure and adopting low-dose CT scans to minimize X-ray exposure. However, these measures affect the diagnostic capabilities of computer-aided diagnosis systems due to the lower CT image quality. In LDCT imaging, noise is often modelled using the Poisson and Gaussian distributions [1], [2], [3], [4], [5], [6], [8], [9], [10], [11]. Removing these noise and artifacts

from LDCT images, techniques are divided into two main categories traditional LDCT denoising methods and deep learning-based approaches. Popular traditional CT images denoising methods like Wavelet-based denoising, BM3D filtering, Dictionary learning, and Non-Local Means algorithms effectively enhance image quality but introduce blurring, struggle with streaking artifacts, or have high computational complexity and potential for artifacts, particularly in regions with high noise levels. Therefore, advanced deep-learning techniques have been introduced.

This SLR categorizes CT denoising models based on deep learning into three distinct and cohesive categories. The first category is the *"Advanced deep learning based denoising techniques*, containing 21 articles from K1 to K21 in Table 8. This category contains on CNNs and their variants, Transformer, and diffusion models.

These algorithms have some promising results but face common challenges, including computational complexity, prolonged training times, and the potential loss of image sharpness. Moreover, the reliance on specific training data and the risk of overfitting are prevalent concerns. Most of the algorithms are evaluated in terms of PSNR and SSIM, which reflects their ability to accurately reconstruct the image PSNR, and preserve the structural details SSIM, but they avoided how much overall error RMSE is minimized. However, some algorithms, like K6 and K21, demonstrate exceptional performance with high PSNR and SSIM values, along with low RMSE, indicating excellent image quality

TABLE 12. Generative adverbial networks (GANs).

References	Methodology / Advantages / Disadvantages	Keys
	Methodology	
References	Advantages	**Keys**
	Disadvantages	
Jiao et al. [74]	The proposed method decomposes LDCT images into frequency components, and a discriminator that utilizes a multi-scale inception structure to evaluate the quality of denoised images.	**K43**
	Accurate reconstruction of denoised images while preserving crucial image features intact.	
	The denoising network has the potential to introduce artifacts or distortions in the denoised images, thereby adversely affecting the overall image quality.	
Yin et al. [75]	The proposed methodology uses an unpaired image-to-image translation framework based on Wasserstein GANs, incorporating the Wasserstein loss into a composite loss function.	**K44**
	LDCT images were denoised without paired training data, improving quality, and preserving features.	
	The training process for Wasserstein GANs can be computationally intensive and time-consuming.	
Li et al. [24]	This method utilizes Cycle GAN, identity GAN, and GAN-CIRCLE, outperforming state-of-the-art methods without requiring paired images.	**K45**
	The proposed method provides a potential solution for improving image quality in a data-efficient manner.	
	Depends on the complexity of the CT images and the specific characteristics of the dataset used for training.	
Marcos et al. [76]	The algorithm utilizes attention and perceptual loss to enhance image quality and preserve crucial details.	**K46**
	Preserved the essential details and improved image quality.	
	Compared to more straightforward denoising methods, the method increases computational complexity and training time.	
Zhang et al.[77]	This paper introduces a multi-scale Res2Net discriminator to enhance the ability to differentiate between real and generated images.	**K47**
	Effectively separates artifacts and noise in LDCT images while preserving edge information.	
	The method requires substantial computational resources and time for training.	
Li et al. [78]	The methodology trains two generators to convert LDCT images to normal doses of CT images and vice versa, ensuring realism through adversarial loss.	**K48**
	The proposed technique improved image quality and preservation of essential details.	
	This method requires a large amount of training data and computational resources" is grammatically correct.	
Park et al. [79]	This section introduces a patch-based GAN method for LDCT denoising and trains a generator function G to approximate clean image distribution and minimize image discrepancies.	**K49**
	The proposed method effectively preserves delicate features and removes noise in LDCT images using unpaired data.	
	This technique's reliance on unpaired data may hinder accurate correspondence capture between noisy and clean CT images, affecting denoising performance.	
Li et al. [80]	This methodology contains the conditional generative adversarial network (CGAN) that effectively handles various unknown noises while preserving image structure.	**K50**
	Accurate reconstruction of denoised images while preserving important image features.	
	The proposed method introduces artifacts or distortions in the denoised images, affecting the overall image quality.	
Chi et al. [81]	This paper uses a modified U-Net structure to enhance the generator with inception-residual blocks and residual mapping.	**K51**
	The proposed method demonstrates superior performance in noise removal, structure preservation, and elimination of false lesions in LDCT images.	
	This method requires significant computational resources and training time due to the complex architecture	
Ma et al. [82]	The method utilizes a noise learning GAN with least squares, structural similarity, and L1 losses for low-dose CT denoising, preserving texture and sharpness.	**K52**
	Removes artifacts in LDCT images while preserving textural details and sharpness.	
	The proposed algorithm still has limitations in handling certain types of noise or artifacts, which could affect the overall performance in specific scenarios.	
Huang et al. [83]	The proposed method, DU-GAN, utilizes U-Net-based discriminators in a GAN framework to learn global and local differences between denoised and normal-dose images in the image and gradient domains.	**K53**
	The proposed network Learned global and local differences, resulting in superior performance compared to current methods.	
	This technique required significant computational resources and training time.	
Kim et al.[84]	This study developed a deep-learning-based image-denoising method for low-dose chest imaging using Conditional Generative Adversarial Networks (CGANs).	**K54**
	This technique improved the Structural Similarity Index Measure (SSIM) by 1.5 to 2.5 times.	
	This method was computationally intensive and time-consuming.	
Yi et al. [85]	The proposed methodology involves two networks: an adversarial-trained network and a sharpness detection network.	**K55**
	This method denoised LDCT images and preserved features with sharpness and detail.	
	This technique trained two networks simultaneously can increase computational complexity and training time.	
Hong et al. [86]	The UIDNet framework employs a cGAN-based noise learning module.	**K56**
	The proposed method achieved high-quality image denoising, without paired clean and noisy images.	
	This method based on cGAN-noise learning module and end-to-end training can increase computational complexity.	

TABLE 12. *(Continued.)* **Generative adverbial networks (GANs).**

Gajera et al. [87]	The methodology focuses on developing an optimized GAN, incorporating novel loss functions, including a Wasserstein adversarial loss and a Charbonnier distance structural loss.	K57
	This method enhanced the denoising performance by leveraging an optimized GAN architecture.	
	This methodology depends on the specific characteristics of the CT scan data and the complexity of the denoising task.	
Bera et al. [88]	The methodology combines a novel convolutional module, a noise-aware loss function, and a unique discriminator function.	K58
	The methodology successfully enhances image interpretability and effectively reduces radiation dose.	
	This technique has the potential requirement for substantial computational resources and time for model training and inference.	
Wang et al. [89]	This study proposes an improved GAN for CT image denoising by enhancing the loss functions and incorporating a composite perceptual loss with noise loss.	K59
	It has enhanced image quality by reducing speckle noise, streaking artifacts, and improving the restoration of visual texture details.	
	The proposed method has potential overfitting of results and has lower values of PSNR and SSIM, which may limit the overall quality assessment of denoised CT images.	
Zhao et al. [90]	The methodology introduces a dual-channel GAN using a separate noise reduction and detail enhancement channel to improve image quality and reduce noise artifacts.	K60
	This method leverages the capabilities of GANs to enhance image quality and reduce noise artifacts.	
	This methodology may require additional computational resources and training time.	
Yang et al. [91]	The methodology introduces a channel-adaptive convolution and patch selection (CAPS) module to enhance feature extraction in low-dose CT denoising.	K61
	It enhanced denoising quality with the utilization of a new wavelet loss function.	
	The utilization of wavelet loss function may affect real-time processing capabilities.	
Yang et al. [92]	The methodology integrates a high-frequency domain U-Net and an image space U-Net within its generator architecture.	K62
	The proposed method precisely handles the high-frequency components for preserving fine details.	
	This method has a potential risk of over-smoothing the image details during the denoising process.	

TABLE 13. **Generative adversarial networks.**

References	Dataset	PSNR	RMSE	SSIM
K43	Mayo Clinic datasets.	27.75	X	0.78
K44	Lung's grand-challenge dataset.	29.7	X	0.69
K45	2016 NIH AAPM-Mayo Clinic Low-Dose CT Grand Challenge.	47.9	X	0.98
K46	Piglet dataset.	33.64	X	0.74
K47		29.26	X	0.71
K48	2016 NIH AAPM-Mayo Clinic Low-Dose CT Grand Challenge.	38.15	X	0.97
K49	Simulated dataset.	34.84	10.46	0.92
K50	Piglet dataset.	34.03	X	0.82
K51	2016 NIH AAPM-Mayo Clinic Low-Dose CT Grand Challenge.	44.4	0.98	0.01
K52		28.49	15.04	0.85
K53		22.31	0.08	0.75
K55	lung-CT-challenge dataset.	26.66	X	0.84
K56	2016 NIH AAPM-Mayo Clinic Low-Dose CT Grand Challenge.	32.48	X	0.9
K58		32.98	9.69	0.91

Where *X denotes that the algorithm hasn't been assessed on that metric.

and accuracy in CT image reconstruction. Others, such as K5 and K9, show discrepancies between the original and reconstructed images despite achieving moderate PSNR and SSIM values. Algorithms like K14 and K15 exhibit low RMSE values, suggesting high accuracy in reconstruction, despite lower PSNR and SSIM values, indicating potential compromises in image quality. The evaluation indicates that the protocols including K6, K7, K14, K15 and K21 have a balanced result in terms of PSNR, SSIM and RMSE. The balanced performance of these algorithms suggests their robustness

and effectiveness in CT image denoising, with consistent preservation of image quality across multiple metrics. While trade-offs may exist between metrics, understanding these trade-offs can guide optimization efforts. Additionally, these algorithms serve as valuable benchmarks for evaluating new techniques and demonstrate potential applicability across various domains, emphasizing the need for standardization in evaluation methodologies.

The second category addressed in this SLR is *Encoder-decoder and U-Net* models as mentioned in Table 10,
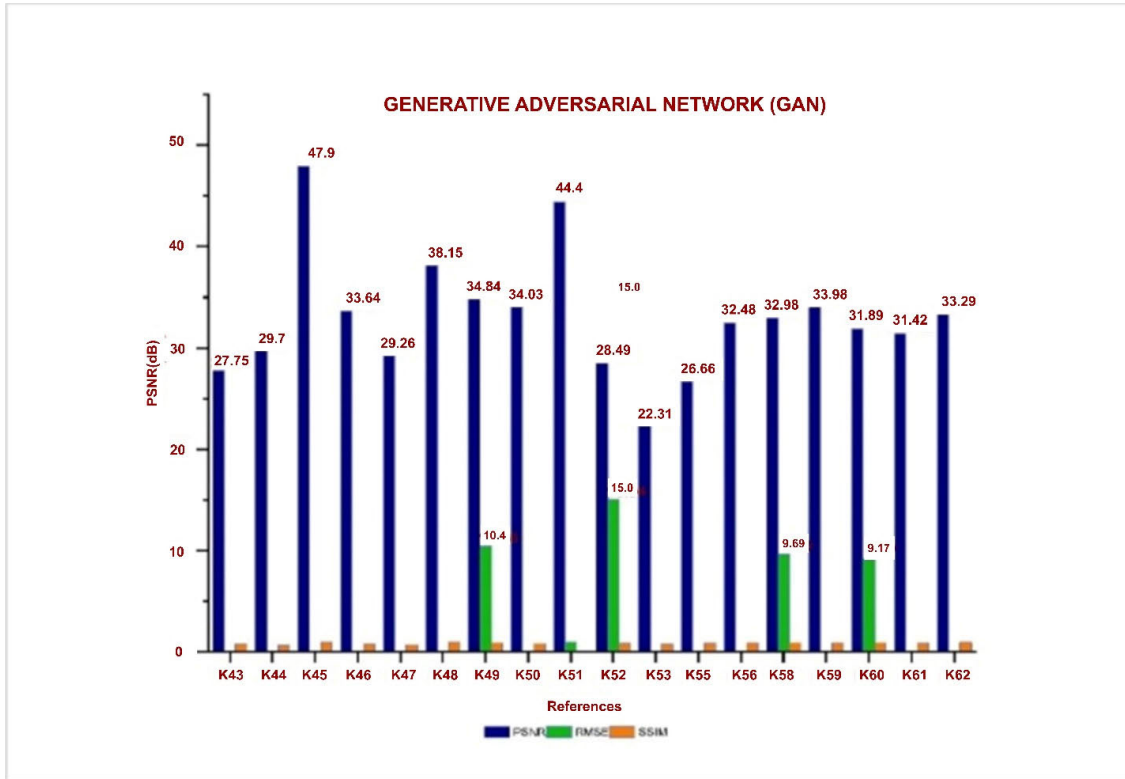
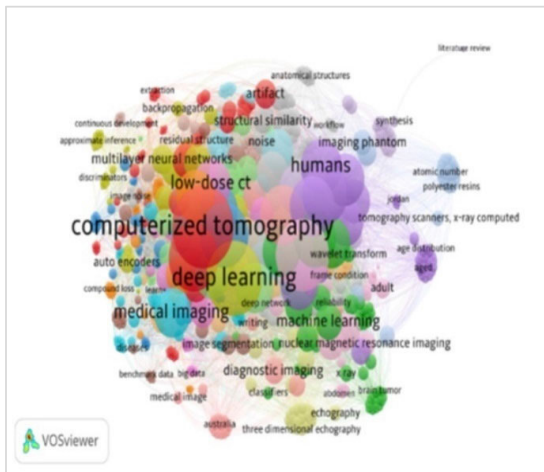**FIGURE 12.** Graphical representation of GANs performance.

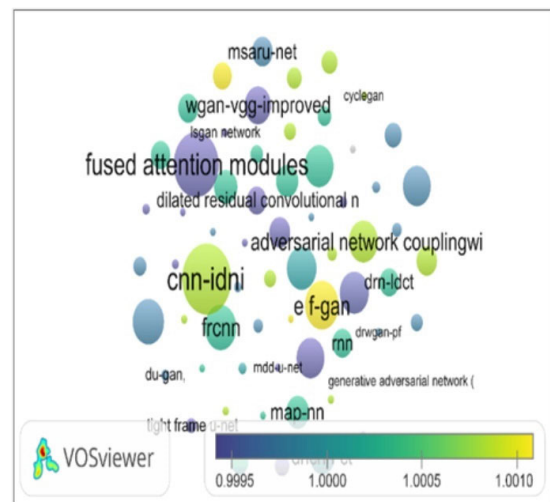**FIGURE 13.** Visualization of keywords.

FIGURE 14. Popular deep learning-based models.

discussed in articles K21 to K42, demonstrate promising capabilities in denoising LDCT images. However, despite their efficacy, these architectures have limitations including the risk of losing fine details, limited adaptability to various noise patterns, potential overfitting, computational complexity, and difficulties in interpretation. Based on PSNR, SSIM, and RMSE metrics, denoising algorithms vary in performance. Algorithms like K28 and K33 excel with high PSNR and SSIM, indicating superior preservation of image quality and low RMSE, implying accurate reconstruction. Conversely, algorithms like K25 and K34 show subpar performance, with low SSIM indicating a significant loss of

structural details. Some strike a balance, like K28 and K29, with high SSIM and low RMSE. However, limitations exist, such as high RMSE in K27, suggesting denoising issues despite moderate PSNR.

The third category discussed in this SLR is *Generative Adversarial Networks (GANs)* algorithms, containing 20 articles from K43 to K62 in Table 12 offer promising capabilities for denoising LDCT images but with certain disadvantages. Firstly, the training process for GANs can be computationally intensive and time-consuming, particularly when dealing
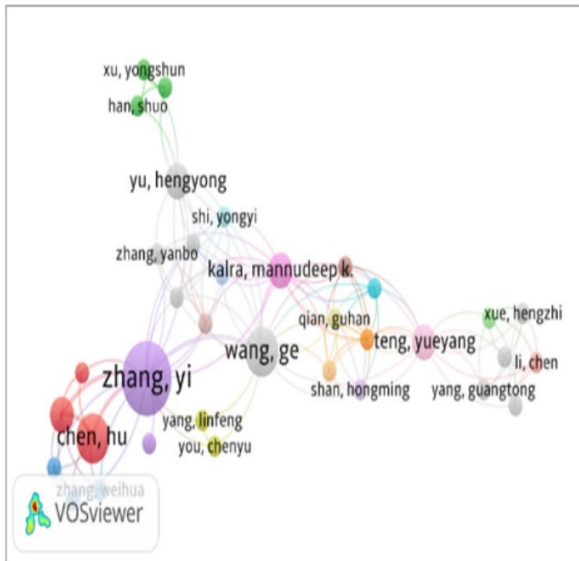
FIGURE 15. Author's connectivity.

with large datasets or complex image structures. Additionally, GANs may introduce artifacts or distortions in denoised images, adversely affecting overall image quality. Moreover, the reliance on unpaired data in some GAN-based methods may hinder accurate correspondence capture between noisy and clean CT images, potentially compromising denoising performance. Lastly, the complexity of GANs architectures poses challenges in interpretation and may limit their practical utility in clinical settings.

The performance of the GAN-based algorithms is also measured in terms of PSNR, SSIM and RMSE. Methods like K45 and K48 showcase impressive SSIM scores, signaling robust preservation of structural information, but may lack in terms of RMSE, potentially indicating a trade-off between noise reduction and image fidelity. On the other hand, methods like K49 and K58 display high RMSE values, suggesting significant discrepancies between denoised and original images, despite relatively high PSNR and SSIM scores. Deep learning models, including CNNs and their variants Transformers, diffusion, autoencoders, U-Net architectures, and Generative Adversarial Networks (GANs), hold promise for LDCT image denoising. These models demonstrate varying degrees of success in preserving image quality while reducing noise. However, they also face common challenges such as computational complexity, prolonged training times, and potential loss of image sharpness. Additionally, the reliance on specific training data and the risk of overfitting are prevalent concerns.

V. FUTURE CHALLENGES
After undergoing a comprehensive study for evaluating various models of LDCT image denoising, several future research directions have been identified.

A. LOSS FUNCTION
Evaluation of LDCT image quality and comparison to reference images involves using diverse metrics. Pixel-wise loss functions utilized for LDCT image denoising can introduce noise and structural distortion, which can blur the images and result in the loss of vital information. To overcome this limitation, potential research can concentrate on developing a cost function that achieves not only precise denoising of LDCT images but also preserves critical features, thereby improving the diagnosis capabilities of the CAD system.

B. LARGE LANGUAGE MODELS (LLMs)
LLMs are a type of artificial intelligence model trained on extensive text data to comprehend and generate human-like text. Models such as GPT and BERT, which are part of this category, utilize transformer architecture and incorporate attention mechanisms to process and analyze language in a contextually relevant manner [95]. These models have been extensively trained on textual data to grasp and generate human-like text, and they can extract semantic features and representations from CT imaging descriptions. By incorporating these features into the loss function, the denoising process can be guided by aligning LDCT images with Normal Dose CT (NDCT) images more effectively [96], [97].

Further, leveraging pre-trained language models enables fine-tuning of medical text data particular to LDCT imaging, allowing for the development of domain-specific representations. Multi-modal fusion approaches, which combine textual information from language models with visual data, further enhance denoising by optimizing alignment between textual and visual representations of CT images. Furthermore, adversarial training approaches incorporate language model-generated text into the loss function, promoting the creation of denoised images that not only physically match NDCT images but also semantically align with textual descriptions.

Finally, including language models in the loss function for LDCT image denoising has tremendous potential to increase the clinical relevance and accuracy of denoised LDCT images, thus boosting medical imaging applications and patient care. Also, the future of LDCT image denoising research involves exploring novel techniques through the integration of LLMs with other deep learning methods or medical imaging techniques. This synergistic approach holds the potential to revolutionize LDCT image denoising, paving the way for enhanced clinical applications and fostering innovation in the field of LDCT imaging.

C. PAIRED DATASET DILEMMA
Further, the availability of an authorized dataset is crucial for training and testing DL-based models. However, many existing algorithms require a paired training dataset, which could be more practical in the case of regular and low-dose

CT scans. It is challenging to match the data accurately due to physical activity, slight variations in scanner position, or patient body movement during scanning, which can adversely affect the denoising performance of the network. Therefore, training DL-based models without paired datasets remains an unresolved issue that requires extensive research. Finding alternative approaches to overcome the lack of paired data is a crucial area of focus for future advancements in this field.

D. STRATEGIC MEMORY OPTIMIZATION

Significant improvements in computing power have enabled the development of more profound and complex DL models for denoising LDCT images, where more extensive and deeper networks can preserve maximum image features. However, the increased depth size of these models and the computational operations involved in convolutional and pooling layers come at the cost of higher computational complexity and memory usage. Consequently, the model's performance may be compromised. Thus, future research can focus on creating models that efficiently handle memory requirements without sacrificing performance to overcome this. This entails exploring novel techniques to optimize computational operations and memory utilization, ensuring effective denoising of LDCT images while maintaining superior performance standards. By pursuing these research directions, further advancements can be made in LDCT image denoising, enabling enhanced image quality, improved diagnostic accuracy, and better utilization of DL techniques.

E. DECENTRALIZED ADVANCEMENTS

Denoising the LDCT scan image to preserve privacy, leverage distributed data, encourage collaboration, enable real-time adaptability, and reduce communication is a task associated with centralized approaches. Federated learning has much potential for the future of LDCT scan image denoising. This decentralized machine learning paradigm enables collaborative model training across IOT-based devices while keeping data localized to resolve privacy problems with medical imaging datasets. Federated learning could help to create robust and generalizable models in the setting of LDCT image denoising by collecting knowledge from varied patient populations and imaging equipment.

VI. CONCLUSION

This systematic literature review extensively investigates the effectiveness of advanced deep learning models: CNNs and their variants, Transformers, Diffusion Encoder-decoder, U-Net, and GANs, for LDCT image denoising. Normal-dose CT scans emit radiation, potentially leading to genetic disorders such as thyroid cancer and leukemia. Consequently, LDCT scans have been introduced, intentionally sacrificing image quality. Traditional LDCT image denoising methods are utilized to enhance LDCT images, however, they often suffer from computational intensity, and vendor dependence and introduce artifacts in flat image regions. Therefore, deep learning based LDCT denoising techniques have emerged.

Furthermore, this study delved into the CT image acquisition process in clinical settings, investigating radiation absorption across different body regions, and identifying noise sources and distribution within LDCT imaging data. Additionally, three research questions are defined regarding advanced deep learning techniques for denoising LDCT images. A total of 62 articles were selected following PRISMA guidelines to address these research questions. According to the report, Google Scholar was the primary source for searching related articles, and the number of publications in this field significantly increased in 2020 and 2021. Moreover, China has emerged as a prominent research contributor in the field of LDCT image denoising, closely followed by the USA, South Korea, and Canada. The primary sources in this SLR were predominantly drawn from IEEE Transactions, with supplementary insights from IEEE conferences and IEEE Access, specifically focusing on CT imaging.

The 2016 NIH AAPM-Mayo Clinic Low-Dose CT Grand Challenge is the primary dataset used, followed by the Cancer Imaging Archive (TCIA), and finally, simulated datasets. These datasets are widely utilized for model training and testing in the CT imaging denoising field. The deep learning-based models with keys K31 and K33 and K36 have shown promising results in terms of SSIM, preserving critical features. Conversely, algorithms K6, K21, K23, K28, K29, and K33, have demonstrated good results in minimizing overall error measured by RMSE. However, it is crucial to achieve a balanced outcome in denoising LDCT images to maintain clinical accuracy, especially concerning metrics such as PSNR, SSIM, and RMSE.

In conclusion, deep learning architectures show promise in denoising LDCT images, but they have some limitations such as the potential loss of fine details, overfitting risks, and computational complexity.

Encoder-decoder and U-Net models show superior results in improving image quality metrics like PSNR, RMSE, and SSIM. However, they have limitations such as potential loss of fine details, difficulties in handling various noise patterns, risk of overfitting, complexity in computation, and interpretation challenges.

Furthermore, although GANs offer effective denoising solutions, concerns arise regarding the introduction of artifacts, accuracy issues due to reliance on unpaired data, and challenges in interpretation. These limitations underscore the need for continued research to address these issues and improve the practical utility of deep learning and GAN-based approaches in clinical settings.

Further, future research directions are to develop a cost function that preserves critical features, explore alternative training approaches for DL models without paired datasets, and optimize computational operations and memory usage in larger models.

Furthermore, leveraging pre-trained language models (LLMs) like GPT and BERT to enhance the alignment between textual descriptions and CT images. This includes incorporating semantic features from LLMs into the denoising process to better match LDCT images with NDCT images. Additionally, multi-modal fusion techniques can be utilized to combine textual information with visual data, moreover, improving denoising outcomes. Adversarial training approaches, integrating language model-generated text into the loss function, hold promise for creating denoised images that align both physically and semantically with NDCT images.

Additionally, Federated learning would be the future of Low-dose image denoising in a decentralized machine learning paradigm. This SLR provides valuable insights into DL techniques for denoising LDCT images. It makes several significant contributions, including identifying research gaps, classification of the literature, evaluation of methodologies, synthesis of findings, critical appraisal of the literature, comparison of results, discussion of practical implications and future research directions. The findings of this SLR significantly enhance the existing knowledge base and extend essential guidance for future research endeavors in the field of LDCT image denoising.

DATA AVAILABILITY STATEMENT
The data supporting this study are available upon request from the corresponding author.

CONFLICT OF INTEREST
The authors declared that they had no conflict of interest.

ACKNOWLEDGMENT

REFERENCES
[1] B. Rusanov, G. M. Hassan, M. Reynolds, M. Sabet, J. Kendrick, P. Rowshanfarzad, and M. Ebert, "Deep learning methods for enhancing cone-beam CT image quality toward adaptive radiation therapy: A systematic review," *Med. Phys.*, vol. 49, no. 9, pp. 6019–6054, Sep. 2022, doi: 10.1002/mp.15840.

[2] A. Heshmatzadeh Behzadi, Z. Farooq, J. H. Newhouse, and M. R. Prince, "MRI and CT contrast media extravasation: A systematic review," *Medicine*, vol. 97, no. 9, p. e0055, 2018, doi: 10.1097/md.0000000000010055.

[3] K. A. S. H. Kulathilake, N. A. Abdullah, A. Q. M. Sabri, and K. W. Lai, "A review on deep learning approaches for low-dose computed tomography restoration," *Complex Intell. Syst.*, vol. 9, no. 3, pp. 2713–2745, Jun. 2023, doi: 10.1007/s40747-021-00405-x.

[4] M. Zhang, S. Gu, and Y. Shi, "The use of deep learning methods in low-dose computed tomography image reconstruction: A systematic review," *Complex Intell. Syst.*, vol. 8, no. 6, pp. 5545–5561, Dec. 2022, doi: 10.1007/s40747-022-00724-7.

[5] A. E. Ilesanmi and T. O. Ilesanmi, "Methods for image denoising using convolutional neural network: A review," *Complex Intell. Syst.*, vol. 7, no. 5, pp. 2179–2198, Oct. 2021, doi: 10.1007/s40747-021-00428-4.

[6] S. Dodia and P. A. Mahesh, "Recent advancements in deep learning based lung cancer detection: A systematic review," *Eng. Appl. Artif. Intell.*, vol. 116, Nov. 2022, Art. no. 105490, doi: 10.1016/j.engappai.2022.105490.

[7] Y.-H. Shao, K. Tsai, S. Kim, Y.-J. Wu, and K. Demissie, "Exposure to tomographic scans and cancer risks," *JNCI Cancer Spectr.*, vol. 4, no. 1, pp. 1–7, Feb. 2020, doi: 10.1093/jncics/pkz072.

[8] M. Diwakar and M. Kumar, "A review on CT image noise and its denoising," *Biomed. Signal Process. Control*, vol. 42, pp. 73–88, Apr. 2018, doi: 10.1016/j.bspc.2018.01.010.

[9] P. Kaur, G. Singh, and P. Kaur, "A review of denoising medical images using machine learning approaches," *Current Med. Imag. Rev.*, vol. 14, no. 5, pp. 675–685, Sep. 2018, doi: 10.2174/1573405613666170428154156.

[10] T. P. Szczykutowicz, G. V. Toia, A. Dhanantwari, and B. Nett, "A review of deep learning CT reconstruction: Concepts, limitations, and promise in clinical practice," *Current Radiol. Rep.*, vol. 10, no. 9, pp. 101–115, Sep. 2022, doi: 10.1007/s40134-022-00399-5.

[11] Z. Zhang and E. Seeram, "The use of artificial intelligence in computed tomography image reconstruction—A literature review," *J. Med. Imag. Radiat. Sci.*, vol. 51, no. 4, pp. 671–677, Dec. 2020, doi: 10.1016/j.jmir.2020.09.001.

[12] G. Tzimas, D. T. Ryan, D. J. Murphy, J. A. Leipsic, and J. D. Dodd, "Cardiovascular CT, MRI, and PET/CT in 2021: Review of key articles," *Radiology*, vol. 305, no. 3, pp. 538–554, Dec. 2022.

[13] K. A. S. H. Kulathilake, N. A. Abdullah, A. Q. M. Sabri, A. M. R. R. Bandara, and K. W. Lai, "A review on self-adaptation approaches and techniques in medical image denoising algorithms," *Multimedia Tools Appl.*, vol. 81, no. 26, pp. 37591–37626, Nov. 2022, doi: 10.1007/s11042-022-13511-w.

[14] H. Ri, J. Kim, M. Lee, H. Hwang, and J. Pak, "Sinogram restoration based on shape property in computed tomography," *Informat. Med. Unlocked*, vol. 20, May 2020, Art. no. 100350, doi: 10.1016/j.imu.2020.100350.

[15] H. Kawashima, K. Ichikawa, K. Matsubara, H. Nagata, T. Takata, and S. Kobayashi, "Quality evaluation of image-based iterative reconstruction for CT: Comparison with hybrid iterative reconstruction," *J. Appl. Clin. Med. Phys.*, vol. 20, no. 6, pp. 199–205, Jun. 2019, doi: 10.1002/acm2.12597.

[16] I. Domingues, G. Pereira, P. Martins, H. Duarte, J. Santos, and P. H. Abreu, "Using deep learning techniques in medical imaging: A systematic review of applications on CT and PET," *Artif. Intell. Rev.*, vol. 53, no. 6, pp. 4093–4160, Aug. 2020, doi: 10.1007/s10462-019-09788-3.

[17] M. A. Gungor, "A comparative study on wavelet denoising for high noisy CT images of COVID-19 disease," *Optik*, vol. 235, Jun. 2021, Art. no. 166652, doi: 10.1016/j.ijleo.2021.166652.

[18] S. Kollem, K. R. L. Reddy, and D. S. Rao, "A review of image denoising and segmentation methods based on medical images," *Int. J. Mach. Learn. Comput.*, vol. 9, no. 3, pp. 288–295, Jun. 2019, doi: 10.18178/ijmlc.2019.9.3.800.

[19] G. L. Zeng, "An attempt of directly filtering the sparse-view CT images by BM3D," in *Proc. 7th Int. Conf. Image Formation X-Ray Comput. Tomogr.*, Oct. 2022, p. 19, doi: 10.1117/12.2646426.

[20] B. K. Shreyamsha Kumar, "Image denoising based on non-local means filter and its method noise thresholding," *Signal, Image Video Process.*, vol. 7, no. 6, pp. 1211–1227, Nov. 2013, doi: 10.1007/s11760-012-0389-y.

[21] M. Unterrainer, C. Eze, H. Ilhan, S. Marschner, O. Roengvoraphoj, N. S. Schmidt-Hegemann, F. Walter, W. G. Kunz, P. M. A. Rosen-schöld, R. Jeraj, N. L. Albert, A. L. Grosu, M. Niyazi, P. Bartenstein, and C. Belka, "Recent advances of PET imaging in clinical radiation oncology," *Radiat. Oncol.*, vol. 15, no. 1, pp. 1–15, Dec. 2020, doi: 10.1186/s13014-020-01519-1.

[22] L. W. Goldman, "Principles of CT: Radiation dose and image quality," *J. Nucl. Med. Technol.*, vol. 35, no. 4, pp. 213–225, Dec. 2007, doi: 10.2967/jnmt.106.037846.

[23] X. Duan, J. Wang, S. Leng, B. Schmidt, T. Allmendinger, K. Grant, T. Flohr, and C. H. McCollough, "Electronic noise in CT detectors: Impact on image noise and artifacts," *Amer. J. Roentgenol.*, vol. 201, no. 4, pp. W626–W632, Oct. 2013, doi: 10.2214/ajr.12.10234.

[24] Z. Li, S. Zhou, J. Huang, L. Yu, and M. Jin, "Investigation of low-dose CT image denoising using unpaired deep learning methods," *IEEE Trans. Radiat. Plasma Med. Sci.*, vol. 5, no. 2, pp. 224–234, Mar. 2021, doi: 10.1109/TRPMS.2020.3007583.

[25] L. N. Fatichah, C. Anam, H. Sutanto, A. Naufal, D. A. Rukmana, and G. Dougherty, "Identification of the computed tomography dose index for tube voltage variations in a polyester-resin phantom," *Appl. Radiat. Isot.*, vol. 192, Feb. 2023, Art. no. 110605, doi: 10.1016/j.apradiso.2022.110605.

[26] Y. Li, Y. Jiang, H. Liu, X. Yu, S. Chen, D. Ma, J. Gao, and Y. Wu, "A phantom study comparing low-dose CT physical image quality from five different CT scanners," *Quant. Imag. Med. Surgery*, vol. 12, no. 1, pp. 766–780, Jan. 2022, doi: 10.21037/qims-21-245.

[27] C. Wohlin, E. Mendes, K. R. Felizardo, and M. Kalinowski, "Guidelines for the search strategy to update systematic literature reviews in software engineering," *Inf. Softw. Technol.*, vol. 127, Nov. 2020, Art. no. 106366, doi: 10.1016/j.infsof.2020.106366.

[28] Y. Xiao and M. Watson, "Guidance on conducting a systematic literature review," *J. Planning Educ. Res.*, vol. 39, no. 1, pp. 93–112, Mar. 2019, doi: 10.1177/0739456x17723971.

[29] J. Zhang, Z. Shangguan, W. Gong, and Y. Cheng, "A novel denoising method for low-dose CT images based on transformer and CNN," *Comput. Biol. Med.*, vol. 163, Sep. 2023, Art. no. 107162, doi: 10.1016/j.compbiomed.2023.107162.

[30] A. Dosovitskiy, L. Beyer, A. Kolesnikov, D. Weissenborn, X. Zhai, T. Unterthiner, M. Dehghani, M. Minderer, G. Heigold, S. Gelly, J. Uszkoreit, and N. Houlsby, "An image is worth 16×16 words: Transformers for image recognition at scale," in *Proc. Int. Conf. Learn. Represent.*, 2021.

[31] F.-A. Croitoru, V. Hondru, R. T. Ionescu, and M. Shah, "Diffusion models in vision: A survey," *IEEE Trans. Pattern Anal. Mach. Intell.*, vol. 45, no. 9, pp. 10850–10869, Jun. 2023, doi: 10.1109/TPAMI.2023.3261988.

[32] H. Shan, A. Padole, F. Homayounieh, U. Kruger, R. D. Khera, C. Nitiwarangkul, M. K. Kalra, and G. Wang, "Competitive performance of a modularized deep neural network compared to commercial algorithms for low-dose CT image reconstruction," *Nature Mach. Intell.*, vol. 1, no. 6, pp. 269–276, Jun. 2019, doi: 10.1038/s42256-019-0057-9.

[33] J. Ming, B. Yi, Y. Zhang, and H. Li, "Low-dose CT image denoising using classification densely connected residual network," *KSII Trans. Internet Inf. Syst.*, vol. 14, no. 6, pp. 2480–2496, 2020, doi: 10.3837/TIIS.2020.06.009.

[34] S. Gou, W. Liu, C. Jiao, H. Liu, Y. Gu, X. Zhang, J. Lee, and L. Jiao, "Gradient regularized convolutional neural networks for low-dose CT image enhancement," *Phys. Med. Biol.*, vol. 64, no. 16, Aug. 2019, Art. no. 165017, doi: 10.1088/1361-6560/ab325e.

[35] M. Gholizadeh-Ansari, J. Alirezaie, and P. Babyn, "Low-dose CT denoising using edge detection layer and perceptual loss," in *Proc. Annu. Int. Conf. IEEE Eng. Med. Biol. Soc. IEEE Eng. Med. Biol. Soc. Annu. Int. Conf.*, Jul. 2019, pp. 6247–6250, doi: 10.1109/EMBC.2019.8857940.

[36] E. Kang, W. Chang, J. Yoo, and J. C. Ye, "Deep convolutional framelet denosing for low-dose CT via wavelet residual network," *IEEE Trans. Med. Imag.*, vol. 37, no. 6, pp. 1358–1369, Jun. 2018, doi: 10.1109/TMI.2018.2823756.

[37] T. Liang, Y. Jin, Y. Li, and T. Wang, "EDCNN: Edge enhancement-based densely connected network with compound loss for low-dose CT denoising," in *Proc. 15th IEEE Int. Conf. Signal Process. (ICSP)*, vol. 1, Dec. 2020, pp. 193–198, doi: 10.1109/ICSP48669.2020.9320928.

[38] Z. Feng, A. Cai, Y. Wang, L. Li, L. Tong, and B. Yan, "Dual residual convolutional neural network (DRCNN) for low-dose CT imaging," *J. Xray. Sci. Technol.*, vol. 29, no. 1, pp. 91–109, 2021.

[39] B. Kim, S. E. Divel, N. J. Pelc, and J. Baek, "A methodology to train a convolutional neural network-based low-dose CT denoiser with an accurate image domain noise insertion technique," *IEEE Access*, vol. 10, pp. 86395–86407, 2022, doi: 10.1109/ACCESS.2022.3198948.

[40] X. Jiang, Y. Jin, and Y. Yao, "Low-dose CT lung images denoising based on multiscale parallel convolution neural network," *Vis. Comput.*, vol. 37, no. 8, pp. 2419–2431, Aug. 2021, doi: 10.1007/s00371-020-01996-1.

[41] H. Song, L. Chen, Y. Cui, Q. Li, Q. Wang, J. Fan, J. Yang, and L. Zhang, "Denoising of MR and CT images using cascaded multi-supervision convolutional neural networks with progressive training," *Neurocomputing*, vol. 469, pp. 354–365, Jan. 2022, doi: 10.1016/j.neucom.2020.10.118.

[42] N. T. Trung, D.-H. Trinh, N. L. Trung, and M. Luong, "Low-dose CT image denoising using deep convolutional neural networks with extended receptive fields," *Signal, Image Video Process.*, vol. 16, no. 7, pp. 1963–1971, Oct. 2022, doi: 10.1007/s11760-022-02157-8.

[43] Z. Chen, C. Niu, Q. Gao, G. Wang, and H. Shan, "LIT-former: Linking in-plane and through-plane transformers for simultaneous CT image denoising and deblurring," *IEEE Trans. Med. Imag.*, vol. 43, no. 5, pp. 1880–1894, May 2024, doi: 10.1109/TMI.2024.3351723.

[44] L. Huang, H. Jiang, S. Li, Z. Bai, and J. Zhang, "Two stage residual CNN for texture denoising and structure enhancement on low dose CT image," *Comput. Methods Programs Biomed.*, vol. 184, Feb. 2020, Art. no. 105115, doi: 10.1016/j.cmpb.2019.105115.

[45] C. You, L. Yang, Y. Zhang, and G. Wang, "Low-dose CT via deep CNN with skip connection and network-in-network," *Proc. SPIE*, vol. 11113, pp. 429–434, Aug. 2019, doi: 10.1117/12.2534960.

[46] M. Chen, Y.-F. Pu, and Y.-C. Bai, "Low-dose CT image denoising using residual convolutional network with fractional TV loss," *Neurocomputing*, vol. 452, pp. 510–520, Sep. 2021, doi: 10.1016/j.neucom.2020.10.004.

[47] A. Zhong, B. Li, N. Luo, Y. Xu, L. Zhou, and X. Zhen, "Image restoration for low-dose CT via transfer learning and residual network," *IEEE Access*, vol. 8, pp. 112078–112091, 2020, doi: 10.1109/ACCESS.2020.3002534.

[48] X. Yang, X. Zheng, Y. Long, and S. Ravishankar, "Learned multi-layer residual sparsifying transform model for low-dose CT reconstruction," 2020, *arXiv:2005.03825*.

[49] Q. Gao, Z. Li, J. Zhang, Y. Zhang, and H. Shan, "CoreDiff: Contextual error-modulated generalized diffusion model for low-dose CT denoising and generalization," *IEEE Trans. Med. Imag.*, vol. 43, no. 2, pp. 745–759, Feb. 2024, doi: 10.1109/TMI.2023.3320812.

[50] D. Yim, B. Kim, and S. Lee, "A deep convolutional neural network for simultaneous denoising and deblurring in computed tomography," *J. Instrum.*, vol. 15, no. 12, pp. P12001–P12001, Dec. 2020, doi: 10.1088/1748-0221/15/12/p12001.

[51] L. Marcos, J. Alirezaie, and P. Babyn, "Low dose CT denoising by ResNet with fused attention modules and integrated loss functions," *Frontiers Signal Process.*, vol. 1, pp. 1–11, Feb. 2022, doi: 10.3389/frsip.2021.812193.

[52] A. Luthra, H. Sulakhe, T. Mittal, A. Iyer, and S. Yadav, "Eformer: Edge enhancement based transformer for medical image denoising," 2021, *arXiv:2109.08044*.

[53] Y. Liu and Y. Zhang, "Low-dose CT restoration via stacked sparse denoising autoencoders," *Neurocomputing*, vol. 284, pp. 80–89, Apr. 2018, doi: 10.1016/j.neucom.2018.01.015.

[54] J. Liu, J. Kang, J. Qiang, Y. Wang, D. Hu, and Y. Chen, "Low-dose CT imaging via cascaded ResUnet with spectrum loss," *Methods*, vol. 202, pp. 78–87, Jun. 2022, doi: 10.1016/j.ymeth.2021.05.005.

[55] Z. Feng, Y. Wang, and A. Cai, "Multi-dimensional spatial attention residual U-Net (Msaru-Net) for low-dose lung CT image restoration," in *Proc. 4th Int. Conf. Adv. Image Process.*, Nov. 2020, pp. 55–60, doi: 10.1145/3441250.3441266.

[56] Z. Feng, Z. Li, A. Cai, L. Li, B. Yan, and L. Tong, "A preliminary study on projection denoising for low-dose CT imaging using modified dual-domain U-Net," in *Proc. 3rd Int. Conf. Artif. Intell. Big Data (ICAIBD)*, May 2020, pp. 223–226, doi: 10.1109/ICAIBD49809.2020.9137456.

[57] Q. Li, S. Li, R. Li, W. Wu, Y. Dong, J. Zhao, Y. Qiang, and R. Aftab, "Low-dose computed tomography image reconstruction via a multistage convolutional neural network with autoencoder perceptual loss network," *Quant. Imag. Med. Surg.*, vol. 12, no. 3, pp. 1929–1957, Mar. 2022, doi: 10.21037/qims-21-465.

[58] J. Zhang, Y. Niu, Z. Shangguan, W. Gong, and Y. Cheng, "A novel denoising method for CT images based on U-Net and multi-attention," *Comput. Biol. Med.*, vol. 152, Jan. 2023, Art. no. 106387, doi: 10.1016/j.compbiomed.2022.106387.

[59] M. Juneja, S. Joshi, N. Singla, S. Ahuja, S. K. Saini, N. Thakur, and P. Jindal, "Denoising of computed tomography using bilateral median based autoencoder network," *Int. J. Imag. Syst. Technol.*, vol. 32, no. 3, pp. 935–955, May 2022, doi: 10.1002/ima.22668.

[60] H. Liu, P. Liao, H. Chen, and Y. Zhang, "ERA-WGAT: Edge-enhanced residual autoencoder with a window-based graph attention convolutional network for low-dose CT denoising," *Biomed. Opt. Exp.*, vol. 13, no. 11, p. 5775, 2022, doi: 10.1364/boe.471340.

[61] M. Zubair, H. B. Md Rais, and Q. Al-Tashi, "U-net autoencoder for edge-preserved denoising of low dose computed tomography images: A novel technique," in *Proc. 13th Int. Conf. Inf. Technol. Asia (CITA)*, Aug. 2023, pp. 19–24, doi: 10.1109/cita58204.2023.10262803.

[62] F. Fan, H. Shan, M. K. Kalra, R. Singh, G. Qian, M. Getzin, Y. Teng, J. Hahn, and G. Wang, "Quadratic autoencoder (Q-AE) for low-dose CT denoising," *IEEE Trans. Med. Imag.*, vol. 39, no. 6, pp. 2035–2050, Jun. 2020, doi: 10.1109/TMI.2019.2963248.

[63] Y. Ma, P. Feng, P. He, Z. Long, and B. Wei, "A deep learning based method for low dose lung CT noise reduction," in *Proc. Chin. Intell. Syst. Conf.* Singapore: Springer, 2019, vol. 592, no. Nov, pp. 649–657, doi: 10.1007/978-981-32-9682-4_68.

[64] D. Wang, Y. Xu, S. Han, and H. Yu, "Masked autoencoders for low dose CT denoising," 2022, arXiv:2210.04944.

[65] M. Zubair, "Enhancing low-dose CT image quality through deep learning: A DoG-sharpened U-Net approach with attention mechanism," in *Proc. ASU Int. Conf. Emerg. Technol. Sustainability Intell. Syst.*, 2024, pp. 1037–1041.

[66] W. El-Shafai, S. Abd El-Nabi, E.-S. M. El-Rabaie, A. M. Ali, N. F. Soliman, A. D. Algarni, and F. E. A. El-Samie, "Efficient deep-learning-based autoencoder denoising approach for medical image diagnosis," *Comput., Mater. Continua*, vol. 70, no. 3, pp. 6107–6125, 2022, doi: 10.32604/cmc.2022.020698.

[67] S. Juliet, "Deep medical image reconstruction with autoencoders using deep Boltzmann machine training," *EAI Endorsed Trans. Pervasive Health Technol.*, vol. 6, no. 24, Dec. 2020, Art. no. 166360, doi: 10.4108/eai.24-9-2020.166360.

[68] C. Yang, J. Ye, Y. Wang, and C. Song, "X-ray breast images denoising method based on the convolutional autoencoder," *Math. Problems Eng.*, vol. 2022, pp. 1–10, Nov. 2022, doi: 10.1155/2022/2362851.

[69] J. Chi, Y. Zhang, X. Yu, Y. Wang, and C. Wu, "Computed tomography (CT) image quality enhancement via a uniform framework integrating noise estimation and super-resolution networks," *Sensors*, vol. 19, no. 15, p. 3348, 2019.

[70] Y. Han and J. C. Ye, "Framing U-Net via deep convolutional framelets: Application to sparse-view CT," *IEEE Trans. Med. Imag.*, vol. 37, no. 6, pp. 1418–1429, Jun. 2018, doi: 10.1109/TMI.2018.2823768.

[71] M. Li, W. Hsu, X. Xie, J. Cong, and W. Gao, "SACNN: Self-attention convolutional neural network for low-dose CT denoising with self-supervised perceptual loss network," *IEEE Trans. Med. Imag.*, vol. 39, no. 7, pp. 2289–2301, Jul. 2020, doi: 10.1109/TMI.2020.2968472.

[72] S. Ramanathan and M. Ramasundaram, "Low-dose CT image reconstruction using vector quantized convolutional autoencoder with perceptual loss," *Sādhanā*, vol. 48, no. 2, pp. 1–5, Mar. 2023, doi: 10.1007/s12046-023-02107-1.

[73] Y. Chai, H. Liu, J. Xu, S. Samtani, Y. Jiang, and H. Liu, "A multi-label classification with an adversarial-based denoising autoencoder for medical image annotation," *ACM Trans. Manage. Inf. Syst.*, vol. 14, no. 2, pp. 1–21, Jun. 2023, doi: 10.1145/3561653.

[74] F. Jiao, Z. Gui, Y. Liu, L. Yao, and P. Zhang, "Low-dose CT image denoising via frequency division and encoder-dual decoder GAN," *Signal, Image Video Process.*, vol. 15, no. 8, pp. 1907–1915, Nov. 2021, doi: 10.1007/s11760-021-01935-0.

[75] Z. Yin, K. Xia, Z. He, J. Zhang, S. Wang, and B. Zu, "Unpaired image denoising via Wasserstein GAN in low-dose CT image with multi-perceptual loss and fidelity loss," *Symmetry*, vol. 13, no. 1, p. 126, Jan. 2021, doi: 10.3390/sym13010126.

[76] L. Marcos, J. Alirezaie, and P. Babyn, "Low dose CT image denoising using boosting attention fusion GAN with perceptual loss," in *Proc. Annu. Int. Conf. IEEE Eng. Med. Biol. Soc.*, 2021, pp. 3407–3410, doi: 10.1109/EMBC46164.2021.9630790.

[77] X. Zhang, Z. Han, H. Shangguan, X. Han, X. Cui, and A. Wang, "Artifact and detail attention generative adversarial networks for low-dose CT denoising," *IEEE Trans. Med. Imag.*, vol. 40, no. 12, pp. 3901–3918, Dec. 2021, doi: 10.1109/TMI.2021.3101616.

[78] Z. Li, J. Huang, L. Yu, Y. Chi, and M. Jin, "Low-dose CT image denoising using cycle-consistent adversarial networks," in *Proc. IEEE Nucl. Sci. Symp. Med. Imaging Conf. NSS/MIC*, Nov. 2019, pp. 1–3, doi: 10.1109/NSS/MIC42101.2019.9059965.

[79] H. S. Park, J. Baek, S. K. You, J. K. Choi, and J. K. Seo, "Unpaired image denoising using a generative adversarial network in X-ray CT," *IEEE Access*, vol. 7, pp. 110414–110425, 2019, doi: 10.1109/ACCESS.2019.2934178.

[80] Z. Li, W. Shi, Q. Xing, Y. Miao, W. He, H. Yang, and Z. Jiang, "Low-dose CT image denoising with improving WGAN and hybrid loss function," *Comput. Math. Methods Med.*, vol. 2021, pp. 1–14, Aug. 2021, doi: 10.1155/2021/2973108.

[81] J. Chi, C. Wu, X. Yu, P. Ji, and H. Chu, "Single low-dose CT image denoising using a generative adversarial network with modified U-Net generator and multi-level discriminator," *IEEE Access*, vol. 8, pp. 133470–133487, 2020, doi: 10.1109/ACCESS.2020.3006512.

[82] Y. Ma, B. Wei, P. Feng, P. He, X. Guo, and G. Wang, "Low-dose CT image denoising using a generative adversarial network with a hybrid loss function for noise learning," *IEEE Access*, vol. 8, pp. 67519–67529, 2020, doi: 10.1109/ACCESS.2020.2986388.

[83] Z. Huang, J. Zhang, Y. Zhang, and H. Shan, "DU-GAN: Generative adversarial networks with dual-domain U-net-based discriminators for low-dose CT denoising," *IEEE Trans. Instrum. Meas.*, vol. 71, pp. 1–12, 2022, doi: 10.1109/TIM.2021.3128703.

[84] H.-J. Kim and D. Lee, "Image denoising with conditional generative adversarial networks (CGAN) in low dose chest images," *Nucl. Instrum. Methods Phys. Res. A, Accel. Spectrom. Detect. Assoc. Equip.*, vol. 954, Feb. 2020, Art. no. 161914, doi: 10.1016/j.nima.2019.02.041.

[85] X. Yi and P. Babyn, "Sharpness-aware low-dose CT denoising using conditional generative adversarial network," *J. Digit. Imag.*, vol. 31, no. 5, pp. 655–669, Oct. 2018.

[86] Z. Hong, X. Fan, T. Jiang, and J. Feng, "End-to-end unpaired image denoising with conditional adversarial networks," in *Proc. AAAI Conf. Artif. Intell.*, Apr. 2020, vol. 34, no. 4, pp. 4140–4149, doi: 10.1609/aaai.v34i04.5834.

[87] B. Gajera, S. R. Kapil, D. Ziaei, J. Mangalagiri, E. Siegel, and D. Chapman, "CT-scan denoising using a charbonnier loss generative adversarial network," *IEEE Access*, vol. 9, pp. 84093–84109, 2021, doi: 10.1109/ACCESS.2021.3087424.

[88] S. Bera and P. K. Biswas, "Noise conscious training of non local neural network powered by self attentive spectral normalized Markovian patch GAN for low dose CT denoising," *IEEE Trans. Med. Imag.*, vol. 40, no. 12, pp. 3663–3673, Dec. 2021. [Online]. Available: https://ieeexplore.ieee.org/stamp/stamp.jsp?arnumber=9474492

[89] X. Wang, J. Wang, and B. Li, "Low dose CT image denoising method based on improved generative adversarial network," in *Proc. 7th Int. Conf. Autom., Control Robot. Eng.*, 2022, pp. 199–203, doi: 10.1109/CACRE54574.2022.9834193.

[90] Y. Zhao, S. Guo, L. Han, and A. Baris Cekderi, "A dual-channel network based GAN for low-dose CT image denoising," in *Proc. China Autom. Congr. (CAC)*, Nov. 2022, pp. 2943–2948.

[91] L. Yang, H. Liu, F. Shang, and Y. Liu, "Adaptive non-local generative adversarial networks for low-dose CT image denoising," in *Proc. IEEE Int. Conf. Acoust., Speech Signal Process. (ICASSP)*, Jun. 2023, pp. 1–5, doi: 10.1109/ICASSP49357.2023.10096998.

[92] L. Yang, H. Shangguan, X. Zhang, A. Wang, and Z. Han, "High-frequency sensitive generative adversarial network for low-dose CT image denoising," *IEEE Access*, vol. 8, pp. 930–943, 2020.

[93] G. Wang, J. C. Ye, and B. De Man, "Deep learning for tomographic image reconstruction," *Nature Mach. Intell.*, vol. 2, no. 12, pp. 737–748, Dec. 2020, doi: 10.1038/s42256-020-00273-z.

[94] Y. Lei, C. Niu, J. Zhang, G. Wang, and H. Shan, "CT image denoising and deblurring with deep learning: Current status and perspectives," *IEEE Trans. Radiat. Plasma Med. Sci.*, vol. 8, no. 2, pp. 153–172, Feb. 2024, doi: 10.1109/TRPMS.2023.3341903.

[95] Z. Chen, T. Chen, C. Wang, C. Niu, G. Wang, and H. Shan, "Low-dose CT denoising with language-engaged dual-space alignment," 2024, arXiv:2403.06128.

[96] Z. Chen, B. Hu, C. Niu, T. Chen, Y. Li, H. Shan, and G. Wang, "IQAGPT: Image quality assessment with vision-language and ChatGPT models," 2023, arXiv:2312.15663.

[97] I. Hartsock and G. Rasool, "Vision-language models for medical report generation and visual question answering: A review," 2024, arXiv:2403.02469.

MUHAMMAD ZUBAIR received the B.Sc. degree in computer science from the University of Peshawar, Pakistan, the MCS. degree from Gomal University, Dera Ismail Khan, and the M.S. degree from Bacha Khan University, Charsadda, Pakistan. He is currently pursuing the Ph.D. degree with Universiti Teknologi PETRONAS (UTP). His professional pursuits revolve around cutting-edge domains, such as machine learning, deep learning, computer vision, medical image processing, algorithm optimization, feature selection, and classification.
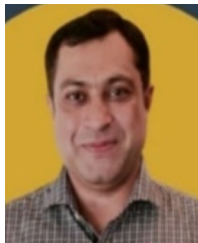
HELMI B. MD RAIS received the B.Sc. degree in science in business administration from Drexel University, USA, the M.Sc. degree in information technology from Griffith University, Australia, and the Ph.D. degree in science and system management from Universiti Kebangsaan Malaysia (UKM). He is currently a Senior Lecturer with Universiti Teknologi PETRONAS. His research interests include ant colony algorithm, optimization, swarm intelligence, and database technologies.

FASEE ULLAH received the degree from the Faculty of Computing, Universiti Teknologi Malaysia (UTM), Malaysia, in 2017. He completed the Postdoctoral Fellowship at the University of Macau in 2021, which is the academic talented program of the Government of Macau. He is currently an Associate Professor with the Department of Computer and Information Sciences, Universiti Teknologi PETRONAS, Malaysia. He has published many research papers in reputed impact factor journals and conferences. His research interests include wireless body area networks, wireless sensor networks, cloud security, smart hash security designing, smart cities, big data analytics, machine learning, deep learning, and the Internet of Things. He was a recipient of the Chancellor Award and the Best Student Award at UTM during the Ph.D. degree, for his excellent research contributions to wireless communication and health monitoring. He is also providing reviewing services to IEEE Transactions on Computers, IEEE Transactions on Network Science and Engineering, IEEE Transactions on Cloud Computing, IEEE Access, IEEE Sensors Journal, ACM, and *International Journal of Distributed Sensor Networks*.

QASEM AL-TASHI received the B.Sc. degree in software engineering from Universiti Teknologi Malaysia (UTM), in 2012, the M.Sc. degree in software engineering from Universiti Kebangsaan Malaysia (UKM), in 2017, and the Ph.D. degree in information technology from Universiti Teknologi PETRONAS, in 2021. He was a Research Scientist with Universiti Teknologi PETRONAS. He was a Postdoctoral Fellow with The University of Texas MD Anderson Cancer Center, Houston, TX, USA, where he is currently a Research Investigator with the Department of Physics. His research interests include feature selection, swarm intelligence, biomarker discovery, survival analysis, multi-objective optimization, and artificial intelligence in healthcare. He is an Editor of the *Journal of Applied Artificial Intelligence* (JAAI) and the *Journal of Information Technology and Computing* (JITC). He is a Reviewer of several high-impact factor journals, such as *Artificial Intelligence Review*, IEEE Access, *Knowledge-Based Systems*, *Soft Computing*, *Journal of Ambient Intelligence and Humanized Computing*, *Applied Soft Computing*, *Neurocomputing*, *Applied Artificial Intelligence*, and *PLOS One*.
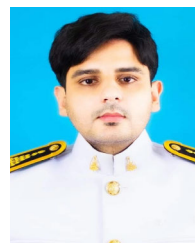
MUHAMMAD FAHEEM received the B.Sc. degree in computer engineering from the University College of Engineering and Technology, Bahauddin Zakariya University (BZU), Multan, Pakistan, in 2010, the M.S. degree in computer science from Universiti Teknologi Malaysia (UTM), Johor Bahru, Malaysia, in 2012, and the Ph.D. degree in computer science from the Faculty of Engineering, UTM, in 2021.
In the past, he was a Lecturer with the COMSATS Institute of Information and Technology, Pakistan, from 2012 to 2014. In addition, he was an Assistant Professor with the Department of Computer Engineering, Abdullah Gü University (AGU), Kayseri, Turkey, from 2014 to 2022. He is currently a Researcher with the School of Computing Science (Innovations and Technology), University of Vaasa, Vaasa, Finland. He has numerous publications in journals and international conferences. His research interests include the areas of cybersecurity, industry 4.0, smart cities, smart grids, and underwater sensor networks.

ARFAT AHMAD KHAN received the B.Eng. degree in electrical engineering from The University of Lahore, Pakistan, in 2013, the M.Eng. degree in electrical engineering from the Government College University Lahore, Pakistan, in 2015, and the Ph.D. degree in telecommunication and computer engineering from the Suranaree University of Technology, Thailand, in 2018. From 2014 to 2016, he was an RF Engineer with Etisalat, United Arab Emirates. From 2018 to 2022, he was a Lecturer and a Senior Researcher with the Suranaree University of Technology. He is currently a Senior Lecturer and a Researcher with Khon Kaen University, Thailand. His research interests include optimization and stochastic processes, channel and the mathematical modeling, wireless sensor networks, ZigBee, green communications, massive MIMO, OFDM, wireless technologies, signal processing, and the advanced wireless communications.

• • •